A CO_2-Silica Geothermometer for Low Temperature Geothermal Resource Assessment, with Application to Resources in the Safford Basin, Arizona

Arizona Geological Survey
Contributed Report 05-B

by

James C. Witcher
and
Claudia Stone

May 2005

This report is preliminary and has not been edited or reviewed for conformity with Arizona Geological Survey standards

Stone and Witcher
Limited Partnership
Consulting Geologists

5933 East Pima Street
Tucson, Arizona 85712

(602) 886-5625

A CO_2-SILICA GEOTHERMOMETER FOR LOW TEMPERATURE GEOTHERMAL RESOURCE ASSESSMENT, WITH APPLICATION TO RESOURCES IN THE SAFFORD BASIN, ARIZONA

BY
JAMES C. WITCHER
AND
CLAUDIA STONE

FINAL REPORT
PREPARED FOR

ARIZONA SOLAR ENERGY COMMISSION
1700 W. WASHINGTON
PHOENIX, ARIZONA 85007

NOVEMBER, 1983

TABLE OF CONTENT

List of Figures i

List of Tables. ii

Introduction. 1
Geothermal Studies. 1
Geothermometers 1
Silica Geothermometers. 1
Previous Studies. 5

Data Collection and Interpretation. 6
Data Sources... 6
Field Water Sampling. 6
Chemical Analyses 7
Drillers' Logs of Well Lithology. 8
Data Processing 9

Background. 12
General Thermodynamic Basis of Chemical Geothermometry. . . 12
The Geochemical System within Basins in the Southwestern U. S. 17
Identification of Factors Affecting the Use of Geothermometers 21
Site Selection for this Study 22

Study Areas 23
Introduction. 23
Physiography and Climate. 23
Historical Geology. 25
Structure 26
Basin-Filling Sediments 29
Cactus Flat-Artesia Subsurface Geology. 31
Buena Vista Subsurface Geology. 36
Geohydrology Cactus Flat-Artesia and Buena Vista. 36
Thermal Regime. 42
Geochemical Model at Cactus Flat-Artesia. 43

Geochemistry. 44
Introduction. 44
Silica Geochemistry 44
Silicate--Water Reactions 48
Carbon Dioxide. 55

Interpretation of Field Studies 57
Interpretation. 57

A CO_2-Corrected Quartz Geothermometer 66

LIST OF FIGURES

Figure No.		Page
1	Stages of basin-fill diagenesis	19
2	Location of study areas	24
3	Map of major structures in the Safford Basin	27
4	Geologic cross section of the Safford Basin	28
5	Location of geologic cross sections at Cactus Flat-Artesia	32
6	Geologic cross section B to B' from Swift Trail to Cactus Flat	33
7	Geologic cross section C to C' from Swift Trail to Artesia	34
8	Geologic cross section D to D' at Cactus Flat	35
9	Map showing elevation tops of the blue clay and inferred structure	38
10	Ground water elevation map at the Cactus Flat-Artesia area	39
11	Distribution of artesian wells in Cactus Flat-Artesia	40
12	Flow rate versus depth of artesian wells	41
13	Solubility of albite expressed as a function of Log $A_{H_4SiO_4}$ versus Log pCO_2 concentration	50
14	Theoretical activity diagram for the system $NaO-Al_2O_3-SiO_2-H_2O$ at 25°C and 1 atmosphere	52
15	Theoretical activity diagram for the system $CaO-MgO-Al_2O_3-SiO_2-CO_2-H_2O$ at 40°C, 1 atmosphere and Log $A_{H_4SiO_4}^{\circ} = -3.54$	58
16	Calcite saturation indices versus total calcium concentration	60
17	Dolomite saturation indices versus total magnesium concentration	61
18	Talc saturation indices versus total magnesium concentration	62
19	Chalcedony saturation indices versus -Log pCO_2 concentration	63
20	Quartz saturation indices versus -Log pCO_2 concentration	65
21	Maps showing Na-K-Ca (upper) and SiO_2 (lower) geothermometer temperatures calculated from published data for Buena Vista	71
22	Map showing Na-K-Ca geothermometer temperatures calculated from published data at Cactus Flat-Artesia	72
23	Map showing SiO_2 geothermometer temperatures calculated from published data at Cactus Flat-Artesia	73
24	Map showing CO_2-corrected quartz geothermometer temperatures, this study, Buena Vista	74
25	Map showing CO_2-corrected quartz geothermometer temperatures, this study, Cactus Flat-Artesia	75

LIST OF TABLES

Table No.		Page
1	Systematics of drillers' log interpretation.	30
2	Formation tops of blue clay unit at Cactus Flat-Artesia	37
3	Analytical expressions relating silica polymorph solubility to temperature	47
4	Measured and geothermometer temperatures, published data, Cactus Flat-Artesia and Buena Vists	70
5	Measured, SiO_2, and pCO_2-corrected geothermometer temperatures, this report, Cactus Flat-Artesia and Buena Vista	76

INTRODUCTION

GEOTHERMAL STUDIES

Geothermics is the study of the earth's heat energy, it's affect on subsurface temperature distribution, it's physical and chemical sources, and it's role in dynamic geologic processes. The term, geothermometry, is applied to the determination of equilibrium temperatures of natural chemical systems, including rock, mineral, and liquid phases. An assemblage of minerals or a chemical system whose phase composition is a function of temperature and pressure can be used as a geothermometer. Thus a geothermometer is useful to determine the formation temperature of rock or the last equilibrium temperature of a flowing aqueous solution such as ground water and hydrothermal fluids.

GEOTHERMOMETERS

Several types of geothermometers exist to determine temperature using analyses aqueous solutions from near-surface (upper crust) environments. They include isotope geothermometers, which are based upon temperature dependent fractionation (Craig, 1953; Lloyd, 1968; Mizutani and Rafter, 1967; McKenzie and Truesdell, 1977; and Ellis and Mahon, 1977) and chemical geothermometers. Commonly used chemical geothermometers fall into one of two categories: (1) cation geothermometers (White, 1963; Ellis and Mahon, 1967; Fournier and Truesdell, 1973; Paces, 1975; Fournier, 1979; Fournier and Potter, 1979; and Benjamin and others, 1983), and (2) silica geothermometers (Bodvarrson, 1960; Fournier and Rowe, 1966; Mahon, 1966; Truesdell, 1976; Fournier, 1973; Fournier, 1977; Fournier, 1981; Fournier and Potter, 1982; and Arnorsson and others, 1983). The subject of this research is silica geothermometers.

Fournier (1981) reviewed evidence for non-quartz control of dissolved silica. This evidence includes (1) anomalously high silica concentrations in natural waters; (2) paragenetic sequences of silica minerals in drill core from geothermal areas; and (3) experimental silica solubility studies that determined of two different silica varieties contact a solution, the more soluble one controls silica concentration. Arnorsson (1975) demonstrated that chalcedony control silica concentrations in Icelandic geothermal systems in basaltic rocks below 110°C and to 180 °C in some cases. To summarize,control of silica concentration in natural waters rests largely upon the silica phase present and upon reaction kinetics (discussed in a later section), in addition to temperature.

In order to successfully apply silica geothermometers to geothermal exploration and reservoir engineering, several models have been developed for their use. These models describe circumstances commonly found in nature. Each model has its own set of requirements, which must hold true if results of geothermometry are to be accurate and reliable. These models are:

(1) The conductive model

If a solution cools conductively (heat loss to country rock) after it leaves a reservoir where it has equilibrated with some polymorphs of silica, it does not lose or gain dissolved silica; it is not mixed with cool near-surface water, or it has not lost steam, a conductive silica geothermometer applies. Conductive silica geothermometers exist for quartz, chalcedony, cristobalite, and opal (Fournier, 1973; Fournier and others, 1974; Fournier, 1977; and Arnorsson, 1983).

(2) The adiabatic model

If a geothermal water has lost steam, the residual silica in solution increases proportional to steam loss. Therefore, the proportion of adiabatic steam loss to conductive cooling is used to correct the silica geothermometer. Adiabatic geothermometers exist for quartz and chalcedony (Fournier and others, 1977; Fournier, 1977; and Arnorsson, 1983). These goethermometers apply to near-surface boiling systems where minimal or no conductive heat loss occurs and no loss of dissolved silica occurs.

(3) Mixing models

Several mixing models exist, which may include the effect of surface boiling (single stage steam loss at a specified enthalpy). The simplest mixing model is hot

aid exploration and developement of the low- to moderate-temperature resources.

PREVIOUS STUDIES

Feth and others (1964) and Garrels and McKenzie (1967) showed that the reactions of dissolved carbon dioxide with primary rock minerals such as feldspars explain the chemical compositions of springs in the Sierra Nevada of California and Nevada. Dissolved silica in these low-temperature waters may be due entirely to acid attack by dissolved carbon dioxide on aluminosilicate minerals, which also releases cations to solution. Busenberg and Clemency (1976) have experimentally determined in long-term tests at standard conditions and constant pCO_2 (1 atmosphere) that silica is initially released rapidly during feldspar-water reactions. However, after several days the silica release rate was very slow and nearly constant. Studies by Rimstidt and Barnes (1980) showed that equilibration rates of silica polymorphs are extremely slow at lower temperatures. Paces (1978) has suggested that aqueous concentrations associated with acid (pCO_2) attack of aluminosilicate minerals are controlled by "hydrodynamic or chemical steady-state mechanisms or through chemical equilibrium with a reversible metastable (aluminum silicate solid." The foregoing studies make it abundantly clear that silica geothermometry at low temperatures (less than 80 C) is fraught with difficulty due to reactions which introduce dissolved silica to solution from non-polymorph sources.

This study investigates silica-water reactions in low-temperature geothermal water in areas near Safford, southeastern Arizona, and derives a pCO_2 correction for conductive silica geothermometers. Use and limitations of the technique are also discussed. Data collection , interpretation approach, and basic geochemistry, as it applies to this study, are outlined. In addition, the geology, thermal regime, geohydrology, and gross geochemistry of the Safford area are reviewed. Finally, geothermal potential, as indicated by this study and previous studies is discussed.

DATA COLLECTION AND INTERPRETATION

DATA SOURCES

Data collected for this study include ground water chemical analyses, drillers' logs of water wells, geohydrologic and geologic information. Published chemical analyses were compiled from Witcher, 1981; Swanberg and others, 1977; Muller and others, 1973; Dutt and McCreary, 1970; and Hem, 1950. Additional analyses from an area near Buena Vista were obtained from a University of Arizona Master's thesis on a sub-economic mineral deposit (Yarter, 1981). Knechtel (1938) published several analyses from the area in a U.S. Geological Survey Water Supply Paper. Knechtel's data were not included in our data base because they were relatively incomplete. Unpublished chemical analyses were obtained from files of the city of Safford's engineers' office and from files of the U. S. Geological Survey, Water Resources Division, Tucson. Because available published and unpublished chemical analyses usually had no aluminum, boron, or lithium analyses and because reliability of pH and alkalinity data were generally unknown, field collection of an additional 42 chemical analyses of ground water was performed.

Drillers' logs and geohydrologic information were obtained from Knechtel, 1938; Witcher, 1982; and from files of the Arizona Department of Water Resources, Phoenix and the U. S. Geological Survey, Water Resources Division, Tucson.

FIELD WATER SAMPLING

Samples were selectively taken from flowing artesian wells except for one pumped well at Buena Vista and one surface runoff sample. Temperature, pH, and total alkalinity were carefully measured in the field in order to obtain the most accurate

than 2 percent. Ion charge balance after speciation calculations, using field pH and alkalinity, were within three percent, except for four samples. Charge balance differences between five and seven percent occurred in three samples; 16W83 was off by 15 percent. Samples 21W83 and 40W83 are from the same well but were collected on different days. Agreement between analyses is better than 96 percent. Thus, the combined effects of sampling error, lab error and changes in discharge chemistry with time are minimal in these two samples.

DRILLERS' LOGS OF WELL LITHOLOGY

Available drillers' logs were compiled to obtain subsurface stratigraphic and structural information. Drillers' logs are difficult to interpret and they may be ambiguous because drillers they usually do not follow geologic convention or vernacular. However, in areas where distinctive lithologic units occur, drillers' logs can be interpreted with a fair degree of confidence. In many cases they provide the only available subsurface information.

Table 1 shows the systematics of drillers'-log interpretation. This method of interpretation is not perfect; but it allows consistent evaluation of the logs. It has been used successfully in the San Simon and Willcox basins (Witcher, 1981; 1982). Units with distinctive color, texture and grain size are generally noted consistently by drillers. In this area, the blue-green clay and sand and gravel descriptions fall into this recognizable category. The blue or green clay is a real unit, which is found in outcrop. Harbour (1966) and White and Smith (1965) indicated that the unit is of lacustrine origin. Witcher (1981; 1982) showed that it occurs as a lens shaped marker bed in the Safford-San Simon basins and the Willcox basin. The blue or green clay thickens toward depositional basin centers; but the blue-green clay elevation tops usually vary only slightly. Perhaps the most difficult stratigraphy to distinguish in drillers' logs is the evaporite sequences within the basins of southeastern Arizona. Geophysical logs and resistivity data are used to supplement drillers' logs when they are available. These methods are sensitive to clay and evaporite sequences (and to ground water with high TDS that is associated with these units). Drillers'-log interpretations are only guides and are not absolutely reliable by themselves. However, their usefulness should not be underestimated; that is why we used them when other information was unavailable.

increases the coefficient deviates more and more from unity.

Calculation of speciation is accomplished by setting up a geochemical model involving mass balance equations similar to Equation 1. Mass action equations are then derived to describe all of the components in the mass balance equations. Using a simplified example from Equation 1, the mass action equations are:

Equation 3

$$K1 = aCaCO3^{\circ} / aCa^{++}\ aCO3^{--}$$

Equation 4

$$K2 = aCaSO4^{\circ} / aCa^{++}\ aSO4^{--}$$

from these equations:

Equation 5

$$mCaCO3o = K1\ aCO3^{--}\ mCa^{++}\ yCa^{++} / yCaCO3^{\circ}$$

Equation 6

$$mCaSO4o = K2\ aSO4^{--}\ mCa^{++}\ yCa^{++} / yCaSO4^{\circ}$$

combining equations 5, 6, and 1:

Equation 7

$$mCa^{++} = mCa^{++}(analyzed) / 1 + yCa^{++}\ (K1\ aCO3^{--} /$$

BACKGROUND

GENERAL THERMODYNAMIC BASIS OF CHEMICAL GEOTHERMOMETRY

Chemical geothermometry is based upon two important concepts describing a chemical reaction. These concepts, chemical equilibrium and reaction kinetics, are best described in terms of energy changes that occur during a chemical reaction. As a reaction proceeds, a point is eventually reached where no net change in energy takes place. At this point a chemical system is in chemical equilibrium. The rate at which a reaction approaches equilibrium is described by reaction kinetics. When a chemical system reaches an equilibrium condition, no net change in energy occurs unless new forces are introduced. Like physical systems in a non-equilibrium condition, chemical systems undergo a spontaneous change until the energy of the system has been minimized. This minimized-energy condition or equilibrium energy is called Gibbs free energy.

Gibbs free energy is a thermodynamic parameter that is used to relate the concentrations of chemical species involved in a reaction. The driving force in a non-equilibrium or initial state that causes a system to change to a final or equilibrium state is called the Gibbs free energy change (G). This parameter commonly employs units of Kcal/mole and is expressed as:

Equation 8

$$G = \triangle G(\text{final}) - \triangle G(\text{initial})$$

In terms of a chemical reaction the Gibbs free energy change may also be written as:

Equation 9

Equation 12

$$\Delta Gr = c\Delta G(C) + d\Delta G(D) - a\Delta G(A) - b\Delta G(B)$$

Inorder to relate Gibbs free energy change of the reaction to standard free energy of formation, equations 10 and 12 are combined and terms rearranged to give:

Equation 13

$$\Delta Gr = \Delta Gf + RT\ln(aC)^{c}(aD)^{d}/(aA)^{a}(aB)^{b}$$

or stated another way:

$$\Delta Gr = \Delta Gf + RT\ln Q$$

Q is a reaction quotient $Q = (aC)^{c}(aD)^{d}/(aA)^{a}(aB)^{b}$

Because a system at equilibrium shows no net energy change, a system at equilibrium at standard state is described as follows:

Equation 14

$$\Delta Gr = 0 = \Delta Gf + RT\ln Q$$

or

$$\Delta Gf = -RT\ln K$$

K is an equilibrium constant

At equilibrium the reaction quotient (Q) equals the equilibrium constant (K). Because geothermometry by definition assumes equilibrium at some specified state, the log ratio Q/K is an important factor to predict how far a reaction has proceeded toward equilibrium and assess the geothermometer reliability in a natural system. This ratio is often referred to as I, an indices of saturation:

Equation 15

$$\log I = \log Q/K$$

concentration is in terms of activity concentration. The relationship between activity concentration, speciation, and measured laboratory concentration is discussed in a later section.

Clearly there are several reactions that have a theoretical potential as geothermometers. However, more is required than temperature dependence of species concentration in a reaction. For a specified reaction to have use, species in the reaction can not be involved in other reactions at faster rates. Just as important, in order that geothermometers have any meaning beyond measured surface conditions, the reaction kinetics must be slow at low temperatures. This slow reaction rate preserves the chemical species concentration after the aqueous solution at equilibrium leaves a reservoir and cools, thus allowing calculation of a reservoir temperature.

Kinetics is described by a general reaction of the form:

Equation 19

$$A + B \underset{kr}{\overset{kf}{\rightleftharpoons}} C + D$$

kf and kr are rate constants

The forward reaction rate (Rf) is described by:

Equation 20

$$Rf = kf[A][B]$$

Brackets denote activity concentration of species A and B.

This relationship is interpreted to show that as a reaction proceeds, the activity concentrations of A and B decrease; likewise Rf , which is initially large, decreases also. The reverse rate (Rr) is described by:

Equation 21

$$Rr = kr[C][D]$$

the geochemical systems found in basins in the southwestern U. S. must first be characterized.

The processes of sediment diagenesis provided general information on basin geochemistry. Diagenesis has been defined by Pettijohn and others (1973) as . . . "all those processes, chemical and physical, which affect the sediment after deposition and up to the lowest grade of metamorphism, the greenschist facies." The overall trend during diagenesis is towards equilibrium, however, equilibrium is usually not reached between all minerals and contained fluids. In an ideal sense, herein lies the main difference between diagenesis and metamorphism. Generally, diagenetic mineral and alteration assemblages only approach equilibrium; whereas metamorphic and hydrothermal assemblages are sometimes interpretable in terms of the assemblage equilibrium at a specified temperature and pressure (Pettijohn and others, 1973). Factors responsible to varying degrees for this difference in overall state of chemical equilibrium are reaction kinetics, time, and fluid-flow rate.

As with hydrothermal and metamorphic processes, diagenetic processes also dramatically change the chemical composition of rocks by chemical mass transport in aqueous solutions. These chemical processes involve both dissolution and precipitation of minerals and cements. Dissolution may be congruent or incongruent. Congruent dissolution removes all components in a solid species into solution. Incongruent dissolution selectively removes a few components to change the composition of a solid. Alteration of feldspars to clay minerals is an example of incongruent dissolution. Precipitation requires that the system is open to fluid flow in order to replenish supersatured solutions. However, with time precipitation of cements and authigenic minerals decreases permeability by filling pore spaces.

Diagenesis of basin-fill sediments in the southwest United States and northern Mexico have been discussed in detail by Walker and others (1978) and Turner (1980). Walker and others (1978) showed that four post-depositional processes affect basin-fill sediments: (1) mechanical infiltration of detrital clay into the interstitial pore spaces; (2) dissolution of primary detrital framework silicate (tectosilicate) minerals; (3) replacement of primary detrital framework silicate minerals by clay; and (4) precipitation of a wide variety of stable and metastable authigenic cementing minerals. These authors noted that these processes are "not equally important everywhere, but almost everywhere one or more of these processes significantly altered the original texture and mineral composition of the sediments." Three stages of diagenesis through time were indentified by Walker and others (1978) (Fig. 1). Stage 1 is infiltration of detrital clay; stage 2 is significant alteration of pyroxene, amphibole and calcium plagiocalse; stage 3 is

complete or nearly complete loss of pyroxene, amphibole and most calcium plagioclase, while potassium feldspar and quartz may show evidence of alteration.

Alteration of primary framework silicate minerals is greatest in minerals low in the Goldich stability series (Goldich, 1938; Loughnan, 1969; Walker and others, 1978; and Turner, 1980). These minerals include plagioclase, augite and hornblende. Dissolution and replacement by clay is the common alteration mechanism.

Walker and others (1978) found that replacement of silicate minerals by clay commonly exceeds 15 percent of the sediment volume and that in most instances this clay is nearly pure montmorillonite.

Most authigenic minerals in the basin-fill sediments are extremely fine grained and normally they are very difficult to recognize without the aid of a scanning electron microscope (Walker and others,1978). Potassiuum feldspar is one of the most common authigenic minerals. Detrital grains of primary potassium feldspar and plagioclase serve as hosts for overgrowths of secondary potassium feldspar. In many locations potassium feldspar crystals are important components of interstitial matrix along with infiltrated clay and authigenic montmorillonite (Walker and others, 1978).

Clinoptilolite, a high-silica zeolite, forms a common cementing material where volcaniclastic detritus occurs. Authigenic potassium feldspar and quartz are commonly associated with this zeolite (Walker and others, 1978). Sheppard and Gude (1973) described the occurrence of zeolite minerals in the Big Sandy formation in western Arizona. Authigenic zeolites are most abundant in altered vitric tuffs and tuffaceous sediments, and may show laterally or vertically zoned zeolite assemblages. Commercial zeolite deposits exist in the Safford-San Simon basin northeast of Bowie, Arizona (Eyde, 1978).

Authigenic montmorillonite is frequently observed in interstitial cavities as small crystals in addition to being a common replacement of alteration minerals (Walker and others, (1978).

Walker and others (1978) found that silica is precipitated as quartz, exhibiting two crystal forms. They stated, "We have not observed the two crystal forms occurring together, and therefore we conclude that one is not the precursor of the other. We also conclude that the two forms reflect either different concentrations of SIO2 in the groundwaters or other differences in the interstitial chemical conditions but we do not know the nature of the differences. Both quartz forms commonly are associated with authigenic potassium feldspar." They further noted that dissoluition of detrital silicate minerals precedes

constant supply of reactive fluid is required. Ground water containing significant quantities of dissolved carbon dioxide is highly reactive with aluminosilicate minerals. The atmosphere and decay of organic material provide the sources for a constant supply of CO_2 in areas of recharging groundwater.

SITE SELECTION FOR THIS STUDY

Two areas near Safford, Arizona were selected for this study. The principal area is south of Safford at Cactus Flat-Artesia. The other is at Buena Vista northeast of Safford.

Major factors for selecting these sites included a knowledge of subsurface temperatures and an understanding of local ground-water geochemistry and the geohydrologic flow system. At Cactus Flat-Artesia these factors have been well characterized. The geochemical, geohydrologic and thermal regimes at Buena Vista are less well known. Another major factor in selecting these sites was that they meet the criteria necessary to adequately study geothermometry. These criteria include:

> (1) distinct, and confined groundwater aquifers. (2) relatively unmixed discharges from the aquifers. (3) relatively wide and predictable subsurface temperature ranges. (4) long term well discharge so that temperature and chemistry best refect aquifer conditions. (5) adequate knowledge of subsurface geology to detail geochemistry and geohydrology.

The Cactus Flat-Artesia area, characterized by numerous thermal and non-thermal flowing artesian wells, meets these criteria very well. While the Buena Vista area has flowing wells, its geologic and geohydrologic conditions are less well known. It was studied primarily to gain more information about the geothermal potential there. Results and conclusions obtained in studies in the Cactus Flat area, therefore, have been applied to assess geothermal resources at Buena Vista.

STUDY AREAS

INTRODUCTION

The two areas investigated during this study lie within the northwest-trending Safford-San Simon basin (Fig. 2). The Cactus Flat-Artesia area straddles U. S. Highway 666 between 8 to 24 km south of Safford. The Buena Vista area encompasses a 16km area northeast of the town of Safford along the Gila River. Both areas have thermal flowing wells with temperatures varying from 35 to 50°C. At present, these waters are utilized in three mineral baths and a catfish farm in the Cactus Flat-Artesia area.

PHYSIOGRAPHY AND CLIMATE

The Cactus Flat-Artesia area is at the base of the Pinaleno Mountains (Fig. 2). Stockton, Marijilda and Graveyard washes, which discharge surface water from deep canyons in the Pinaleno Mountains, have dissected the area into a succession of mesas, fans, and arroyos. Flow occurs during winter and early spring due to snow melt at high elevations. All drainage flows north and east toward the Gila Valley.

The impressive Pinaleno Mountains rise abruptly to form a range over 3,300m in elevation, where more than 76cm/yr of precipitation falls. The Cactus Flat area lies at 900 to 1,100m elevation and receives only 20 to 25cm of precipitation annually. Because of high mean annual temperature (17 °C) and thick stands of tamarisk trees, evapotranspiration is high in this area.

The Buena Vista area is in the Gila River flood plain at an elevation of 910 to 920m. West of Buena Vista, the flood plain widens and curves northwestward south of Safford to form a

flat-bottomed valley 5 to 8km across (Fig. 2). Eastward, the flood plain narrows into the northeast-trending Gila Box, a canyon formed by the Gila River between the Gila Mountains and the Peloncillo Mountains. Paired terraces 20 to 30m high bound the flood plain. Above the terraces 5 to 20km-wide piedmonts slope gently upward toward the Gila and Peloncillo Mountains except north of Buena Vista where at least two more older ancestral Gila River terraces are found. Mean annual temperature is 17°C and precipitation is less than 25cm/yr. The Gila River is a perennial stream at this location.

HISTORICAL GEOLOGY

The crust of this region is highly anisotropic and is dominated by a west-northwest structural grain, which is superimposed on an older northeast grain (Swan, 1982; Silver, 1978). This anisotropicity originated during the Precambrian. During the Mesozoic, tectonism reactivated structures to create a highland that crosses the Safford region (Coney, 1978; Turner, 1962; Elston, 1958). Major erosion, resulting from uplift, removed Paleozoic and pre-Late Cretaceous rocks to expose Precambrian basement. Late Cretaceous shales and sandstones were deposited over the Precambrian terrane (Elston, 1958). Later, Paleocene (Laramide) volcanism and plutonism was active in the area. Laramide andesitic flows and silicic stocks crop out in the Gila Mountains and are associated with economic copper mineralization (Dunn, 1978). The Eocene was an interval of erosion and local sedimentation, probably accompanying major tectonism and a break in volcanism. During this time copper mineralization was unroofed in the Gila Mountains, and Late Cretaceous shales were partially removed. Late Oligocene and early Miocene volcanism buried the area in basaltic and andesitic flows and volcanoclastic sediment up to 1km thick (Strangway and others, 1976; Richter and others, 1981). Limited silicic volcanism occurred as rhyolitic-dacitic domes and associated pyroclastic deposits in the vents and on margins of large stratovolcanoes and along major structural lineaments. No major silicic cauldrons, such as those found in southwestern New Mexico and in the Chiricahua Mountains, Arizona, have been observed in the Safford area. However, silicic mid-Tertiary plutons were emplaced in the Pinaleno Mountains (Thorman, 1981). During Miocene, crustal extension began to form the proto Basin and Range. This normal faulting was characterized in places by listric style rotation of upper crustal fault blocks, overlying low angle decollements at depth. Local sedimentation accompanied this tectonism. Low angle faults are sometimes closely related spacially and

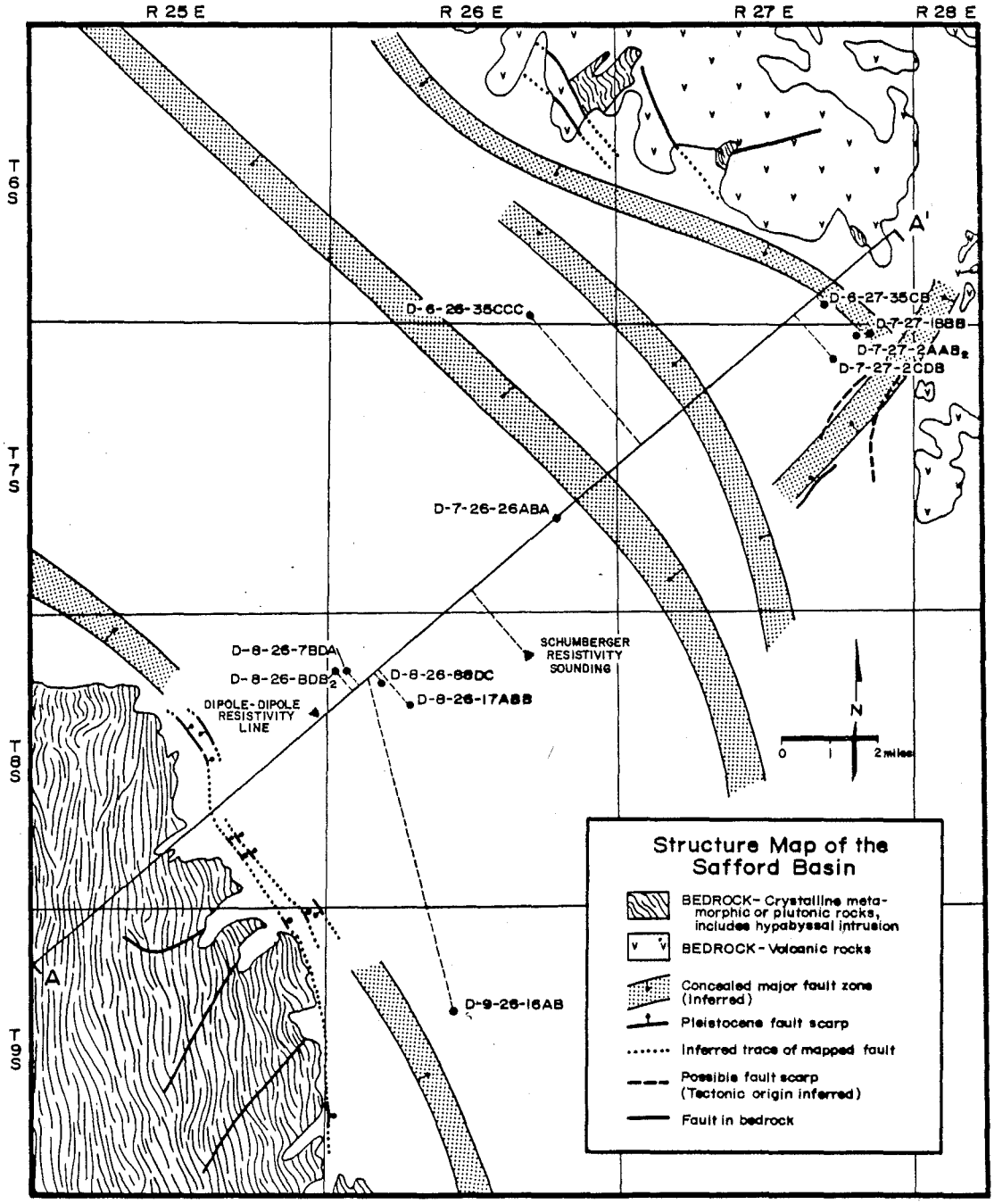

Figure 3 Map of major structures in the Safford Basin

others,1982).

Bedrock (noncontinental clastic rocks) includes mostly schist, gneiss, granite, quartzitic mylonite, andesitic to basaltic volcanic rocks and minor rhyolitic to dacitic volcanic rocks. Mineralogy of these units includes common aluminosilicate minerals, hornblende, augite, biotite, chlorite and feldspars. Volcanic minerals probably comprise olivine, chalcedony, cristobalite, zeolites and calcite. Quartz is common to all units. Rocks associated with Laramide copper mineralization also contain kaolinite, sericite, epidote, chlorite, gypsum and anhydrite.

Sediments filling the contemporary Safford basin are over 1,220m thick and they indicate several distinct depositional environments. In general, but not always, the fine_grained and evaporite sediments are found toward the basin center and away from the margins. Basin-filling units are probably most important in this study because nearly all water sampled during this study has been confined to these formations. Water in the Buena Vista area is a possible exception; it may have flowed upward from underlying bedrock.

BASIN-FILLING SEDIMENTS

Harbour (1966) divided the basin-fill into two major units, upper and lower basin fill. These units are separated by a time-stratigraphic horizon that shows a change in sedimentation processes(fluvial-lacustrine-playa to fluvial-alluvial) and by a Pliocene to Quaternary faunal transition. Harbour (1966) also divided the basin-fill sediments into facies. Because drillers' logs were used in our subsurface interpretations, we have generalized Harbour's units in to three major groups. Table 1 shows the correlation of our stratigraphic units with those of Harbour and gives the systematics of drillers'-logs interpretation within our stratigraphic divisions. We used the following stratigraphic subdivisions: (1) a sand-conglomerate facies, (2) a silt-clay facies, and (3) an evaporite facies. We have divided the silt-clay facies into two sub-units: (1) a blue or green clay unit, and (2) a brown-yellow silt and clay. All of the facies intertongue.

The silt-clay facies is lacustrine (blue-green clay) and fluvial over-bank (blue-green clay, in part, and the yellow-brown silt and clay unit). The evaporite facies consists of gypsiferous clay, gypsum, anhydrite, and halite and it was

deposited in a playa environment. In a few areas the top of the silt-clay facies consists of a zone of gypsiferous, limonitic and calcareous clay. These deposits may indicate desiccation of the Pliocene lake. Air-fall ash deposits are common in the upper silt-clay facies and they are commonly zeolitized, diatomaceous, or argillic and calcareous. Harbour (1966) suggested the most common basin-fill clay mineral is montmorillonite.

Upper basin-fill consists of mostly gruslike sand with gravel lenses, except north of Buena Vista, where fine grained tuffaceous sediments are interbedded in sandy and silty sediments adjacent to the Gila Mountains.

A thin generally less than 20m-thick cobble to boulder conglomerate caps the basin-fill deposits to form Pleistocene to Recent geomorphic surfaces. These sediments are pediment caps, ancestral Gila River terrace deposits, and alluvial fan deposits. Ancestral Gila River gravels are usually well rounded dark volcanic clasts with a few well rounded red granite clasts (Morenci Granite?).

Calcite is the most common cement in upper basin fill and in degradational deposits. Harbour (1966) stated that coarse upper basin-fill units frequently show "replacement" of hornblende and plagioclase by sparry calcite. Other minerals such as quartz and orthoclase may show "corrosion" by calcite. Harbour also described two unusual forms of interstitial calcite: spherolitic cementation, and sand-calcite crystals.

CACTUS FLAT-ARTESIA SUBSURFACE GEOLOGY

We have inferred subsurface geology has been inferredfrom drillers' logs. Figure 5 shows the locations of cross sections in Figures 6, 7, and 8. Cross section B-B' from Swift Trail to Cactus Flat shows the blue clay unit pinching out to the south and fine grained units becoming dominate at Cactus Flat. Cross section C-C' is from Swift Trail to Artesia. The blue clay pinches out to the west and silt-clay is dominant towards Artesia. Cross section D-D' is from west to east across the Cactus Flat area. Drillers' logs were used to infer structure also, which is somewhat speculative. However, the high total dissolved solids in wells in this area could result from contact with the gypsiferous sediments (evaporites) that we have interpreted to be faulted upward in a narrow horst block in this area (also see Figure 9). This structural interpretation is based upon blue clay elevation tops and the top of the evaporite

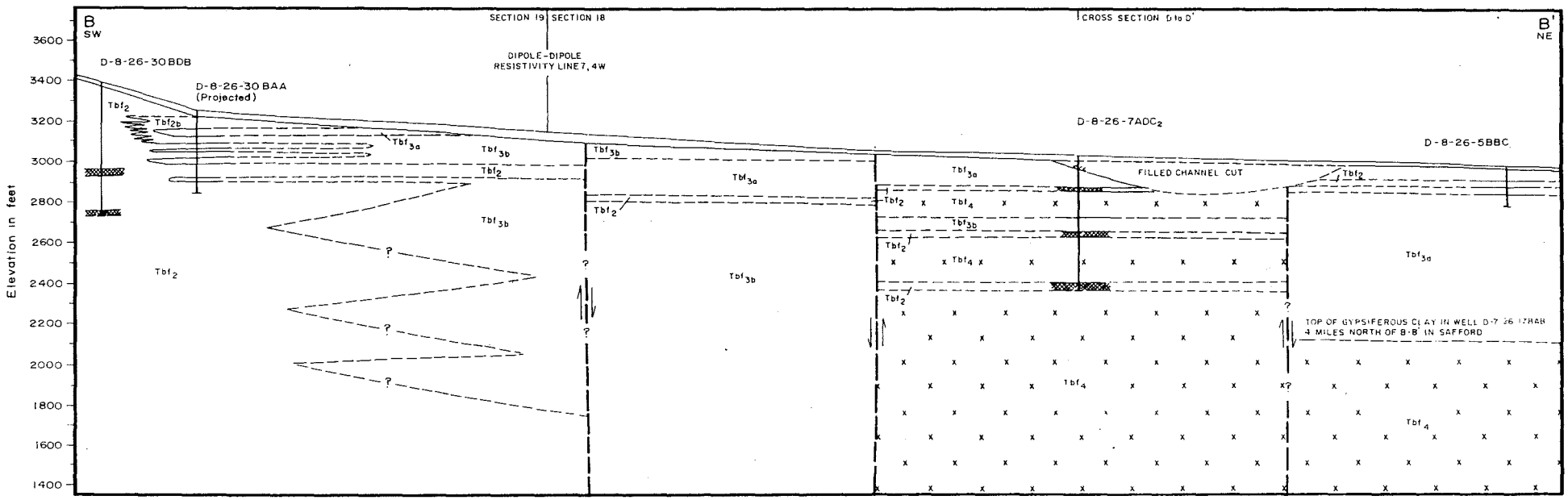

EXPLANATION

- Tbf_2 — Sand/conglomerate facies
- Tbf_{3a} — Silt/blue clay facies
- Tbf_{3b} — Silt/brown clay facies
- Tbf_4 — Evaporative facies
- WATER

Figure 6 Geologic cross section B to B' from Swift Trail to Cactus Flat

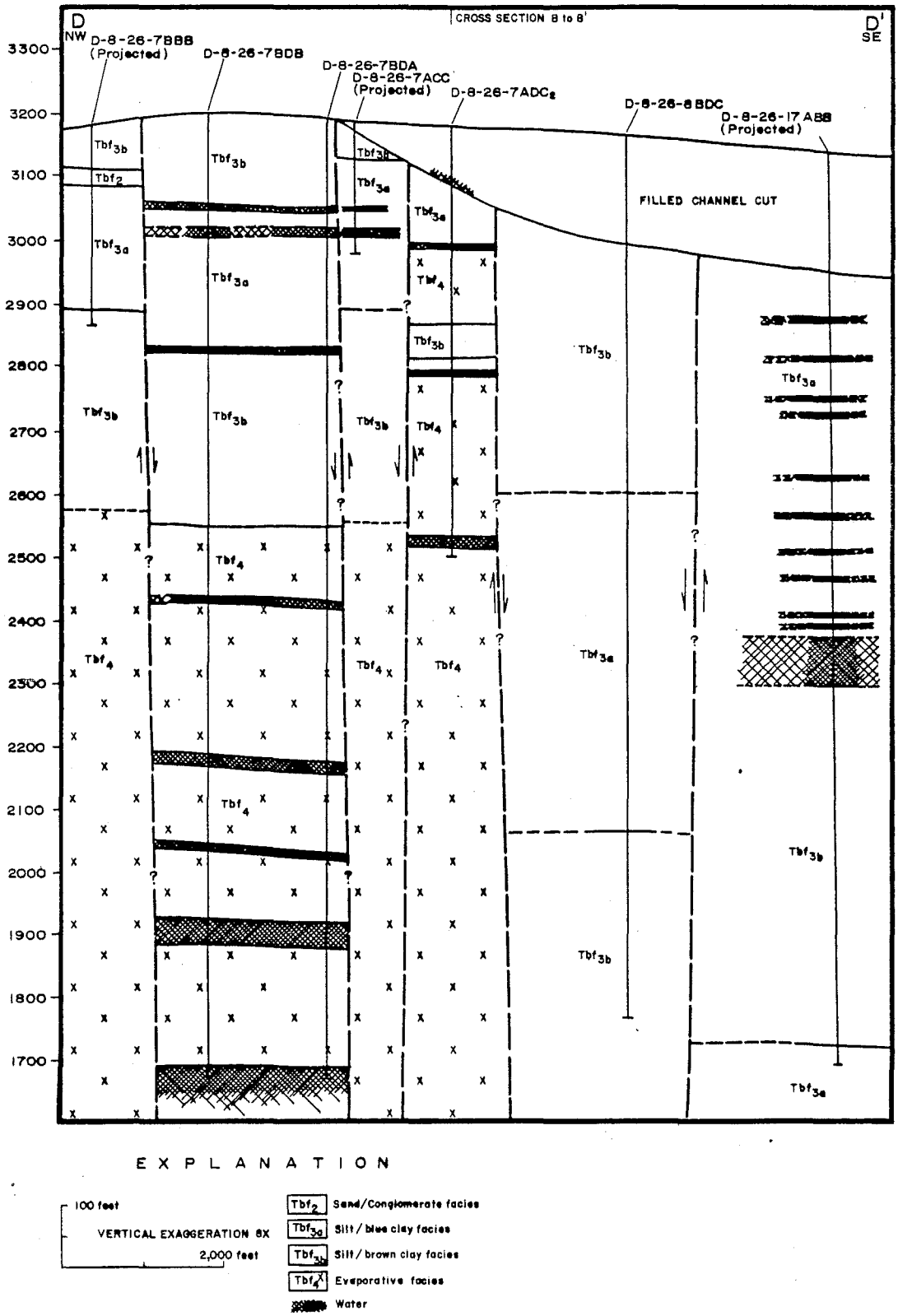

Figure 8 Geologic cross section D to D' at Cactus Flat

TABLE 2 - Formation tops of blue clay unit at Cactus Flat-Artesia

No.	Well Location	Elevation	Top Blue Clay (Depth)	Top Blue Clay (Elevation)
1	(D-8-26) 5bbc	3,100'	148'	2,952'
2	(D-8-26) 6ccb	3,200'	115'	3,085'
3	(D-8-26) 7acc	3,170'	48'	3,122'
4	(D-8-26) 7adc$_2$	3,160'	81'	3,079'
5	(D-8-26) 7bbb	3,180'	80'	3,100'
6	(D-8-26) 7bcc$_2$	3,190'	40'	3,115'
7	(D-8-26) 7bda	3,180'	269'	2,911'
8	(D-8-26) 7bdb$_2$	3,200'	269'	2,931'
9	(D-8-26) 8bdc	3,160'	557'	2,603'
10	(D-8-26) 17abb	3,130'	190'	2,940'
11	(D-8-26) 17bbc	3,180'	565'	2,615'
12	(D-8-26) 21cdc	3,210'	101'	3,109'
13	(D-8-26) 28dbb	3,230'	81'	3,149'
14	(D-8-26) 30aca	3,342'	60'	3,282'
15	(D-8-26) 30baa	3,350'	80'	3,270'

data (less than 100m) (U. S. Geological Survey, WRD, Tucson). Shallow unconfined ground water flows generally toward the north and north-northeast as does surface drainage. The water table gradient is about 100 feet per mile. A small ground-water depression exists at Artesia, which may result from drawdown due to heavy pumping.

Artesian wells occur in a 3-km-wide arc, which mimics the Pinaleno Mountain front. This arc is between 3 and 4km from the mountain front (Fig. 11). We believe the arcuate distribution of the artesian wells is a result of sand-conglomerate tongues in the silt-clay and evaporite facies, rather than fault-induced geohydrologic processes. The convergence of topography and hydraulic head in sand and gravel aquifers is of primary importance in allowing flow from these wells. Flow rates from the artesian wells increase systematically with depth (Fig. 12). This fact suggests that several distinct and confined aquifers exist and that hydraulic pressure also increases with depth.

Several flowing wells and pumped artesian wells discharge thermal water (>35 °C) at Buena Vista. Pumped flow rates exceed 1,000 gpm (U. S. Geological Survey, WRD, Tucson). This water is produced from sand-conglomerate facies that are confined below

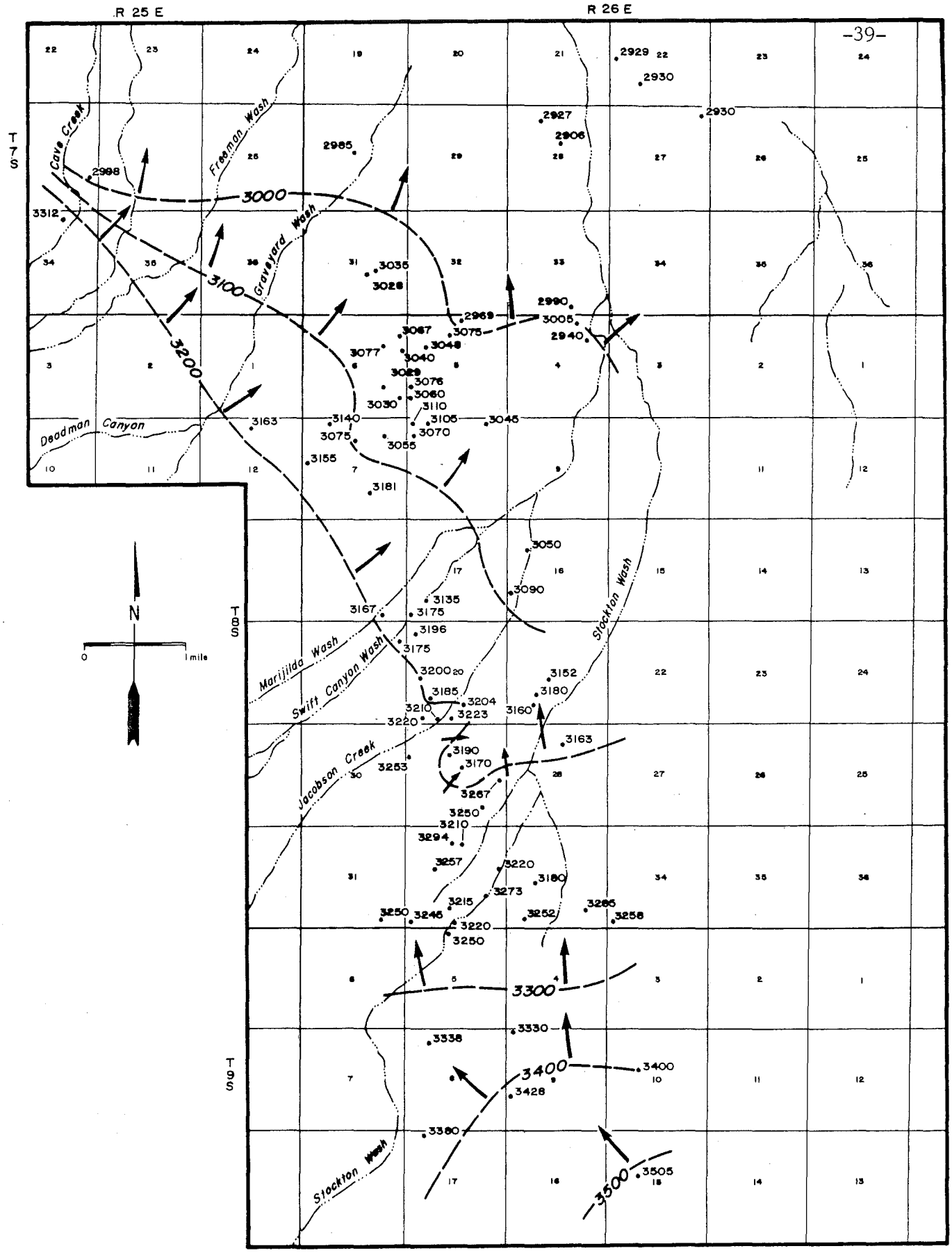

Figure 10 Ground water elevation map at the Cactus Flat- Artesia area

(Water table elevation for wells less than 160 feet in depth)

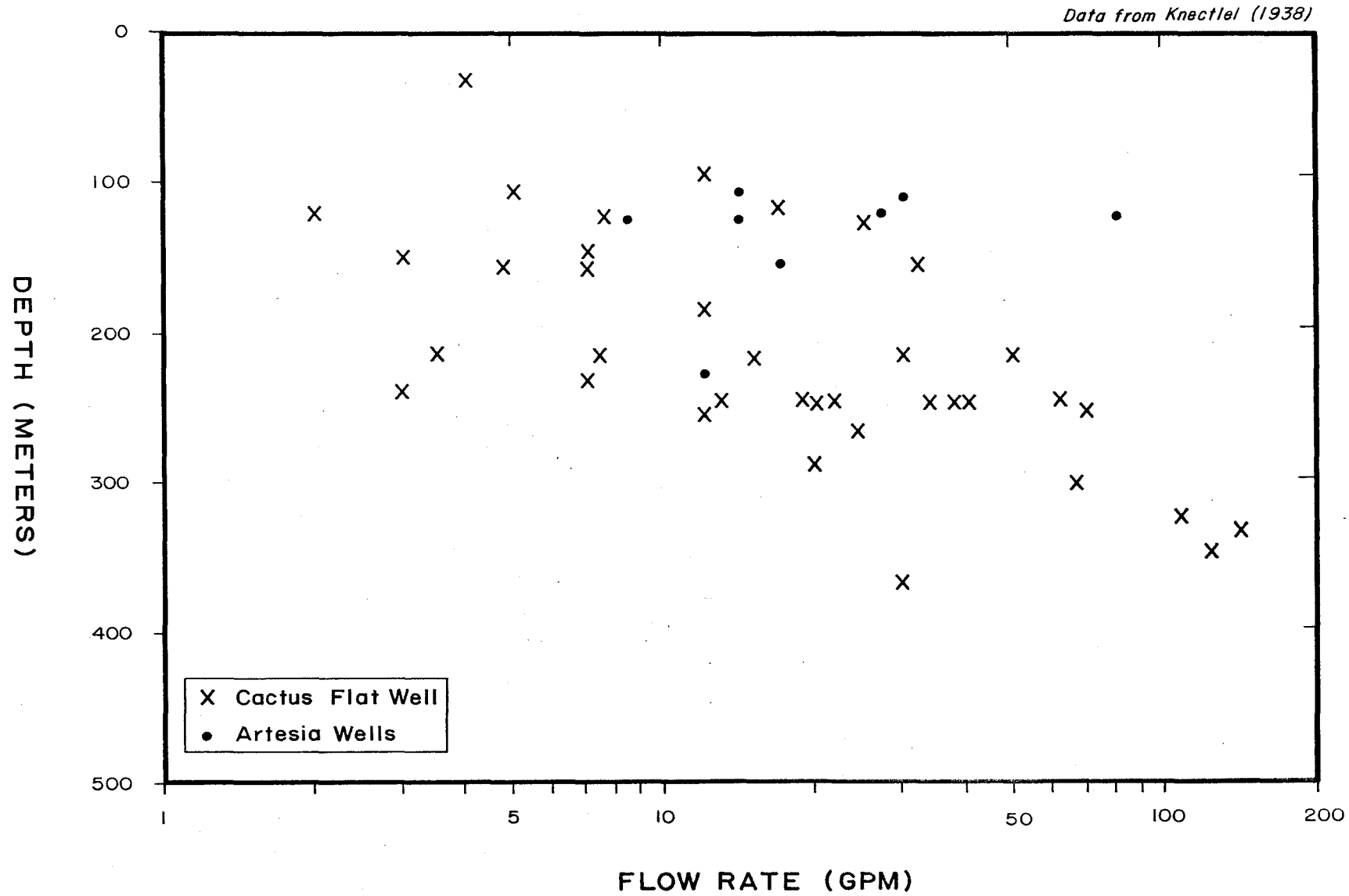

Figure 12 Flow rate versus depth of artesian wells

GEOCHEMICAL MODEL AT CACTUS FLAT-ARTESIA

Cold (<30°C) ground water in the Cactus Flat area has generally sodium sulfate-bicarbonate chemistry with TDS less than 1,000 ppm. Thermal water (>30°C) has sodium chloride-sulfate chemistry with TDS between 1,000 and 9,000 ppm. Witcher(1981) showed that the milliequivalent chloride-sulfate versus bicarbonate ratio has a logarithmic relation to the milliequivalent lithium concentration. This correlation suggests that thermal and nonthermal water chemistry evolves from contact with differing rocks through equlilibria and (or) ion exchange processes. The silt-clay and evaporite facies provide a source for sulfate, chloride, and lithium.

Silica concentrations are frequently highest in nonthermal, sodium bicarbonate waters. Also, unusually warm waters near Artesia do not deviate from these observations and their gross chemistry trends are indistinct from other waters in the Cactus Flat-Artesia area. The following geochemical model applies in the Cactus Flat area. Meteoric water recharging aquifers near the Pinaleno Mountain front has high dissolved carbon dioxide content, which attacks aluminosilicate minerals to form sodium-bicarbonate water. As ground water flows deeper into and laterally through sand and gravel zones confined by silt-clay and evaporite sequences, gypsum, halite, and carbonate minerals dissolve. Solution of evaporites and ion exchange with clay minerals occurs to transform the sodium bicarbonate water into sulfate-chloride water.

GEOCHEMISTRY

INTRODUCTION

The geochemical discussion presented in the following section focuses on mineral-water thermodynamic processes and how they relate to silica concentration and dissolved carbon dioxide. In a previous section the rates of chemical processes were discussed in terms of reaction kinetics from a thermodynamic standpoint. Hydrodynamic factors are equally important in overall kinetics of natural systems. Hydrodynamic factors involve the flow paths, contact time, and nature of the interface between minerals and solutions. In-depth discussion of these factors are found in Berner (1978, 1980), Freeze and Cherry (1979), Dominico (1977), and Paces (1976). In this report these factors are not discussed except where they grossly influence thermodynamic processes.

SILICA GEOCHEMISTRY

Dissolved silica solutions that become supersaturated with respect to opal are unique compared to most other inorganic solutions because silica tends to polymerize and stay in solution as colloidal particles and gels (Iler, 1979). However, at concentrations usually encountered in low temperature waters, silica occurs as a monomeric species rather than in a multimeric form. Studies by Alexander and others (1954) have shown that the colored complex, formed by silico-molybdate colorimetric measurements of aqueous silica, results from monomeric silicic acid ($H_4SiO_4^\circ$). Solid silica polymorphs dissolve in water to produce this species.

$$SiO_2(qtz) + 2H_2O = H_4SiO_4^\circ$$

The solubility constant (K_{qtz}) for this reaction is:

Equation 29

$$mH_4SiO_4^{\circ} = SiO_2(\text{measured as molality})/[1 + yH_4SiO_4^{\circ}(K_1 10^{pH}/yH_3SiO_4^- + K_1K_2 10^{2pH}/yH_2SiO_4^{--})]$$

where:

Yi = activity coefficient of species i
mi = molal concentration of species i

Analytical expressions that may be used to calculate K and K at any temperature are:

Equation 30

K1 = -2549/T - 15.36 X 10E-6 TE2 (Arnorsson and others, 1982)

Equation 31

K2 = 5.37 - 3320/T - 20 X 10E-3 T (Arnorsson and others, 1982)

where:

T = absolute temperature in degrees Kelvin

Constants K1 and K2 used in the WATSPEC program are determined using analytical expressions given by Truesdell and Jones (1974). Quartz solubilities have been measured experimentally over a wide range of temperatures and pressures in both pure water and in salt solutions. Fournier and Potter (1982) and Fournier (1983) have reviewed these experiments and provided additional experimental solubility information. Table 3 lists several analytical expressions from recent literature relating quartz solubilities to temperature.

Experimental solubilities of other polymorphic forms of silica are found in Kennedy (1950), Alexander and others (1954), Siever (1962), Krauskopf (1956), Fournier (1973), Fournier and Rowe (1977), Rimstidt and Barnes (1981), and Fournier and Marshall (1983). The empirical solubility of chalcedony based on geothermal wells in Iceland was given by Arnorsson and others (1983). Table 3 lists analytical expressions relating various silica polymorph phase solubilities to temperature.

The kinetics of silica-water reactions were reported in terms of interfacial area and water mass by Rimstidt and Barnes (1981). They reported that reverse rate (precipitation) constants of all silica phases are the same at a specified temperature. However,

the forward rate (dissolution) constants vary depending upon the polymorphic phase present at a particular temperature. Reaction rates are faster at higher temperatures and slower at lower temperatures. One practical aspect of the Rimstidt and Barnes (1981) work is,

> "Upon cooling a silica-saturated solution below the equilibrium temperature, the decreasing solubility causes increasing supersaturation, which tends to raise the precipitation rate, but the rate constants rapidly decrease, which tends to lower the precipitation rate. These competing effects cause a maximum rate of precipitation 25-50 °C below the saturation temperature. At temperatures below that of the maximum rate, silica is often quenched into solution by very slow reaction rates. Consequently, the quartz geothermometer will give the most accurate results if samples are taken from the hottest, highest flow rate, thermal springs which occur above highly fracture areas."

A parallel conclusion drawn by these authors is that due to fast reaction rates above 150 °C, quartz geothermometers work best on systems whose reservoir temperatures are below 200 °C. In systems near or above 200 °C, significant precipitation of quartz is highly probable, as the waters cool and flow through the 150 to 200 °C temperature zones on the margins of high temperature systems.

In conclusion, the congruent dissolution (and precipitation) reaction rates of silica polymorphs are very slow at low temperatures. Where very fine grained particles or crystals of the polymorphs exist, reaction rates are faster and solubilities are apparently higher.

SILICATE-WATER REACTIONS

So far discussion has shown that silica polymorphs in contact with water are sources of dissolved monomeric silicic acid. Another large group of water-mineral reactions also releases $H_4SiO_4^{\circ}$ to solution. Studies by Feth and others (1964) were among the first to dramatically detail these sources of H_4SiO_4 in low temperature water. Feth and others (1964) in studies of low temperature and thermal springs in the Sierra Nevada of

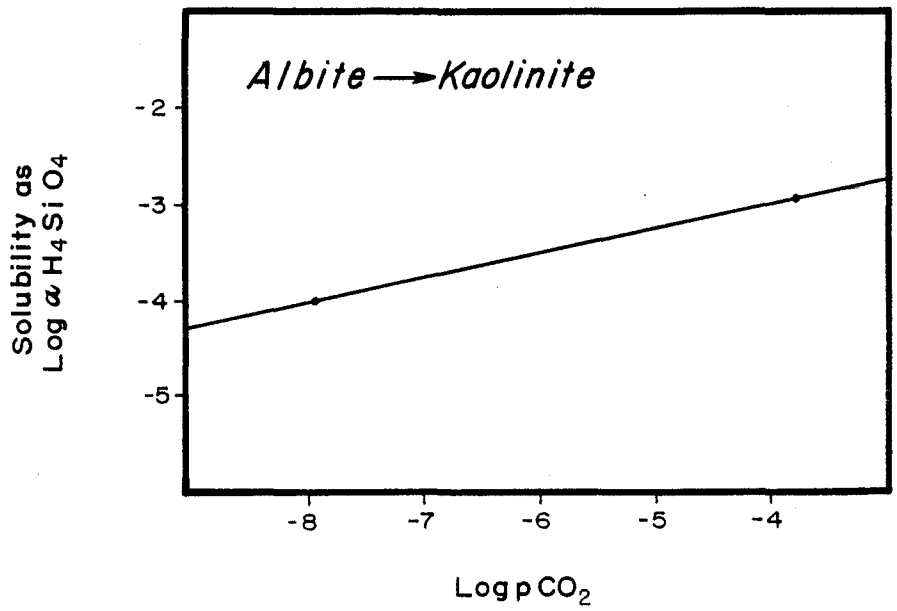

Figure 13 Solubility of albite expressed as a function of Log $A_{H_4SiO_4}$ versus Log pCO_2 concentration

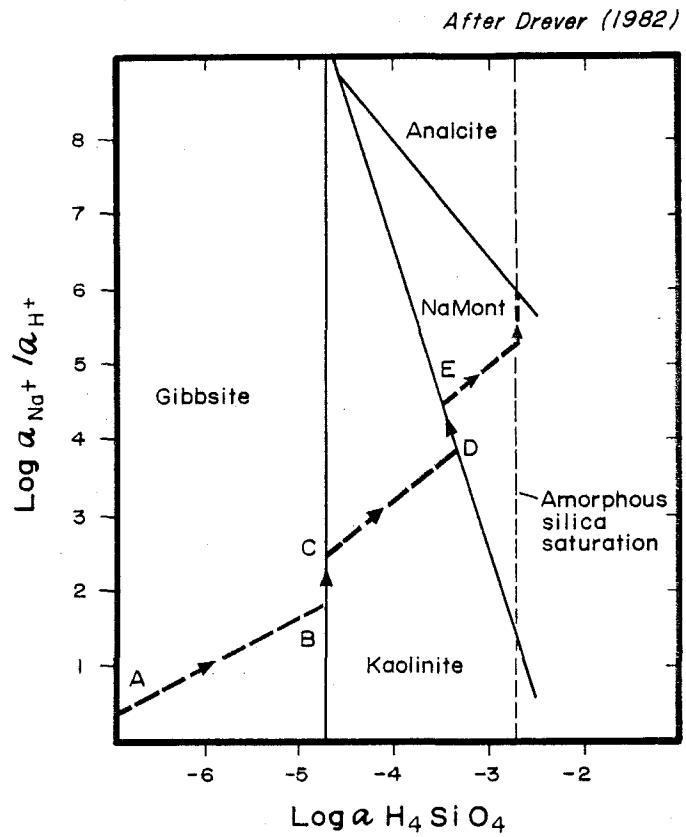

Figure 14 Theoretical activity diagram for the system $NaO-Al_2O_3-SiO_2-H_2O$ at 25°C and 1 atmosphere. Diagram shows predicted path or evolution of solution as albite reacts with water (after Drever, 1982).

> "...although Berner and Holdren explained well the rate of dissolution of silicates, their mechanism does not directly explain the stoichiometry. In experiments of Busenberg and Clemency (1976), and in those of Luce and others (1972), cations appeared in solution at a more rapid rate than silica, implying that a silica-rich residue must exist somewhere."

Models presented by Paces (1978, 1973) may best explain the low silica release rate, compared to cations, and solid conservation of aluminum, during linear rate law release. Paces (1978, 1973) proposed that an amorphous metastable reversible aluminum silicate whose composition varies with pH controls silica concentration rather than a strictly irreversible and incongruent dissolution model, such as was previously discussed in this study using a stability diagram and albite reactions. Whether or not Paces' hypothesized metastable aluminumsilicate forms a diffusive surface layer, which controls early cation release, is apparently highly uncertain.

Other interesting results of feldspar reaction experiments are also pertinent to this study. Bailey (1976) showed that higher temperatures increase the linear rate kinetics of incongruent silicate dissolution. Results of Busenberg and Clemency (1976) indicate that the different feldspar phases have linear rate kinetics at a particular temperature and pCO_2, which are within an order of magnitude of one another. Finally, Paces (1973) and Wildman and others (1968) showed that incongruent solubility of silicate minerals is also a function of pCO_2 in natural systems.

Regardless of the exact nature of aluminum silicate dissolution, the following conclusions are evident from the literature:

> (1) Both temperature and pCO_2 have a significant effect on silicate mineral solubility. (2) pH of waters in terranes comprised of silicic rocks is buffered by dissolution of primary silicate minerals. (3) $H_4SiO_4^{\circ}$ in low temperature water in contact with silicic rocks is largely due to incongruent disslolution and possibly steady-state equilibrium with various stable and metastable alteration products such as magnesium silicates, zeolites, clay minerals, and aluminum silicates. The effect of silica polymorph control on $H_4SiO_4^{\circ}$ concentration may increase with higher temperature and (or) lower pCO_2.

subsurface. Calcite and dolomite precipitation are additional subsurface sources of pCO_2. This process is not a net gain in carbonate to the system.

Equation 41

$$Ca^{++} + 2HCO_3^- = CaCO_3 + CO_2 + H_2O$$

Details of carbonate chemistry are discussed in Garrels and Christ (1965) along with common ion effects of gypsum dissolution on carbonate equilibria.

INTERPRETATION OF FIELD STUDIES

INTERPRETATION

Geochemical theories and laboratory experiments reported in the literature concerning the relations between aluminosilicate minerals and carbon dioxide rich waters were tested and applied to the chemistry of ground water collected from the Safford area.

Examination of mineral saturation indices caculated by the WATSPEC program reveals that calcite ($CaCO_3$), talc ($Mg_3Si_4O_{10}(OH)_2$), and quartz (SiO_2)are routinely saturated or supersaturated. Dolomite ($CaMg(CO_3)_2$, chalcedony (SiO_2), chlorite ($Mg_3Al_2Si_3O_{10}(OH)_8$), and aragonite ($CaCO_3$) are sometimes supersaturated, but they are usually slightly undersaturated to saturated. Adularia ($KAlSi_3O_8$), albite ($NaAlSi_3O_8$), Ca-montmorillonite ($Ca_{0.167}Al_{2.33}Si_{3.67}O_{10}(OH)_2$), and kaolinite ($Al_2Si_2O_5(OH)_4$) are generally slightly saturated to undersaturated. Mineral equilibrium was indicated if the indices were within -+ 5 percent of the mineral equilibrium constant, taken from Truesdell and Jones (1974). Minerals in equilibrium with Safford area ground water are consistent with the mineralogy of basin-fill sediments. Where aluminum concentration was below the unit of reliable quantitative analyses, indices for aluminosilicate minerals were not calcualted by WATSPEC.

Since montmorillonite is a ubiquitous mineral in basin-fill sediments, ground-water chemistry was plotted on an activity-activity diagram showing the stability fields for Mg-montmorillonite, Ca-montmorillonite, and kaolinite (Fig.15). This diagram allows interpretation of various components of the ground-water chemistry with respect to mineral phases. Calcite and dolomite saturation surfaces at a particular pCO_2 were plotted as a function of aCa^{++}/a^2H^+ (Drever, 1982). The saturation surfaces of talc and sepiolite were plotted as a function of aMg^{++}/a^2H^+. Solubility constants for these magnesium silicates were calculated from thermodynamic data tabulated in Drever (1982).

Most sampled ground water falls into the Mg-montmorillonite stability field. Four samples plot in the kaolinite field; the remaining samples plot in the Ca-montmorillonite field. Sample 22, which plots in the middle-left portion of the kaolinite field, is surface snow-melt flow from Marijilda Wash. This sample is representative of recharge water before it reacts with soil and near surface sediments and enters the ground-water system. As recharge water reacts with subsurface rocks it loses pCO_2 and increases in pH through loss of H^+ to silicate alteration minerals. Since talc and sepiolite are apparently saturated, they may control magnesium (and silica) concentration at pH greater than 8.5 and at lower pCO_2 ($-\log pCO_2 > 3.8$). At lower pH and higher pCO_2 concentrations, dolomite is the more stable mineral phase.

Comparison of the calcite saturation indices with total calcium concentration dramatically shows that calcite equilibrium controls total calcium concentration (Fig. 16). Nearly all samples plot within the bounds of calcite saturation. Figure 17 is a plot of dolomite saturation indices versus total magnesium concentration in parts per million. Generally, concentrations above 0.6 ppm are controlled by dolomite equilibrium. The small number of samples in apparent supersaturation with calcite are in eqilibrium with dolomite. Samples that plot in the Ca-montmorillonite stability field and in the Mg-montmorillonite field above a line drawn between samples 12 and 7, are undersaturated with dolomite. Due to the low magnesium concentration in these waters, another magnesium mineral(s) is suspected to control magnesium concentration in the dolomite-undersaturated water.

Talc saturation indices were plotted against total magnesium concentration in Figure 18. Samples that were undersaturated with dolomite approach gross equilibrium with talc. Waters with magnesium concentration greater than 1.0 ppm are either in equilibrium or supersaturated with talc. Samples with magnesium concentration less than 0.6 ppm fall into two general groupings. One group approaches gross equilibrium; the other group is in a field approaching supersaturation. The latter group may actually have attained equilibrium with sepiolite. These relationships suggest that magnesium silicates control very low (<0.6 ppm) magnesium concentrations. Magnesium silicate solubility control of dissolved magnesium and silica at high pH has been suggested by the field and laboratory studies of Klein (1974) in the San Luis basin, Colorado and by the laboratory experiments of Siffert (1962). For completeness, it should be noted that if a sepiolite equilibria phase exists, it is metastable because talc and dolomite are more stable.

Figure 19 is a plot of pCO_2 versus chalcedony saturation indices. It is generally believed by most workers that chalcedony controls silica concentration in waters below 100 C.

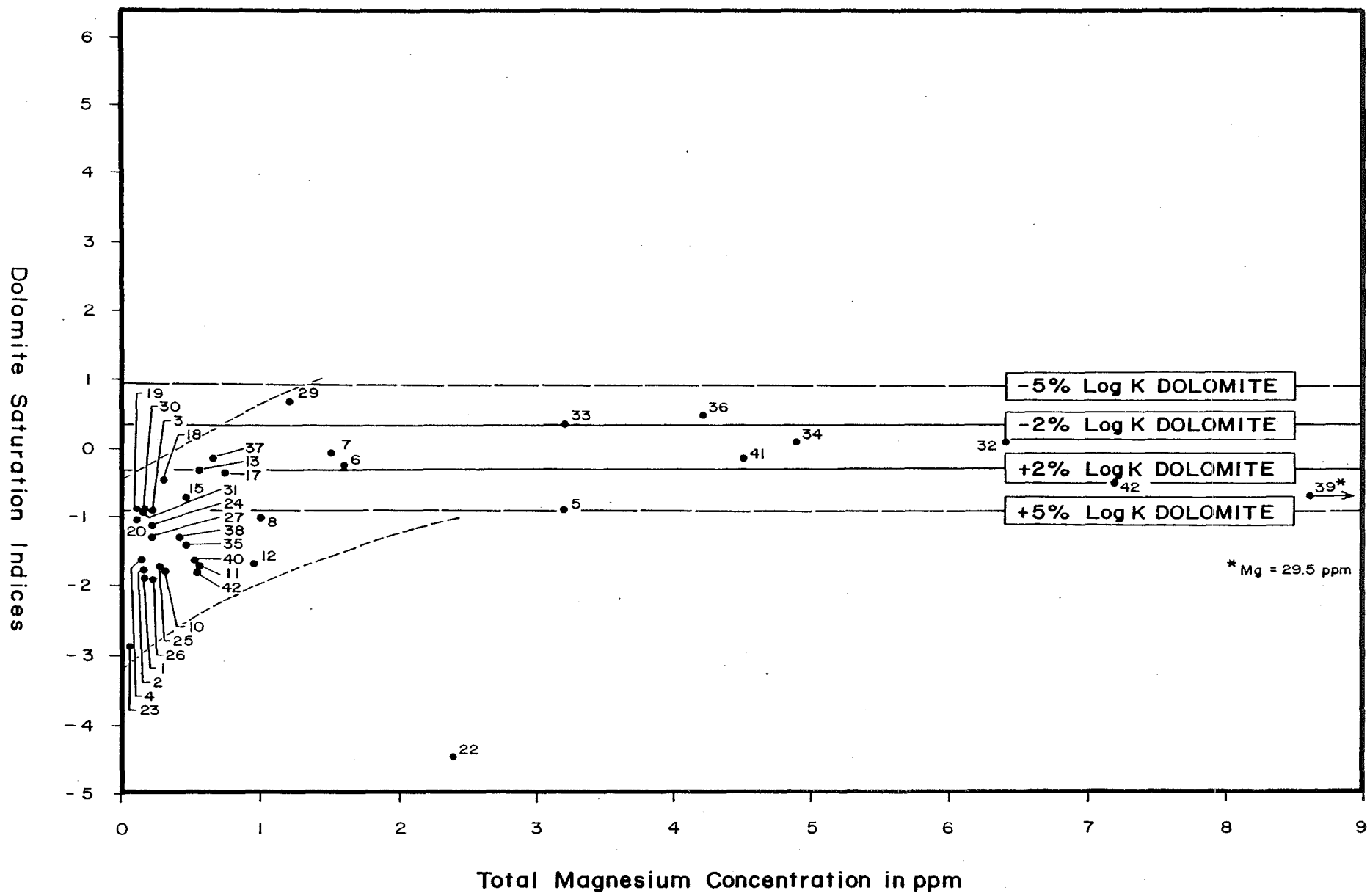

Figure 17 Dolomite saturation indices versus total magnesium concentration

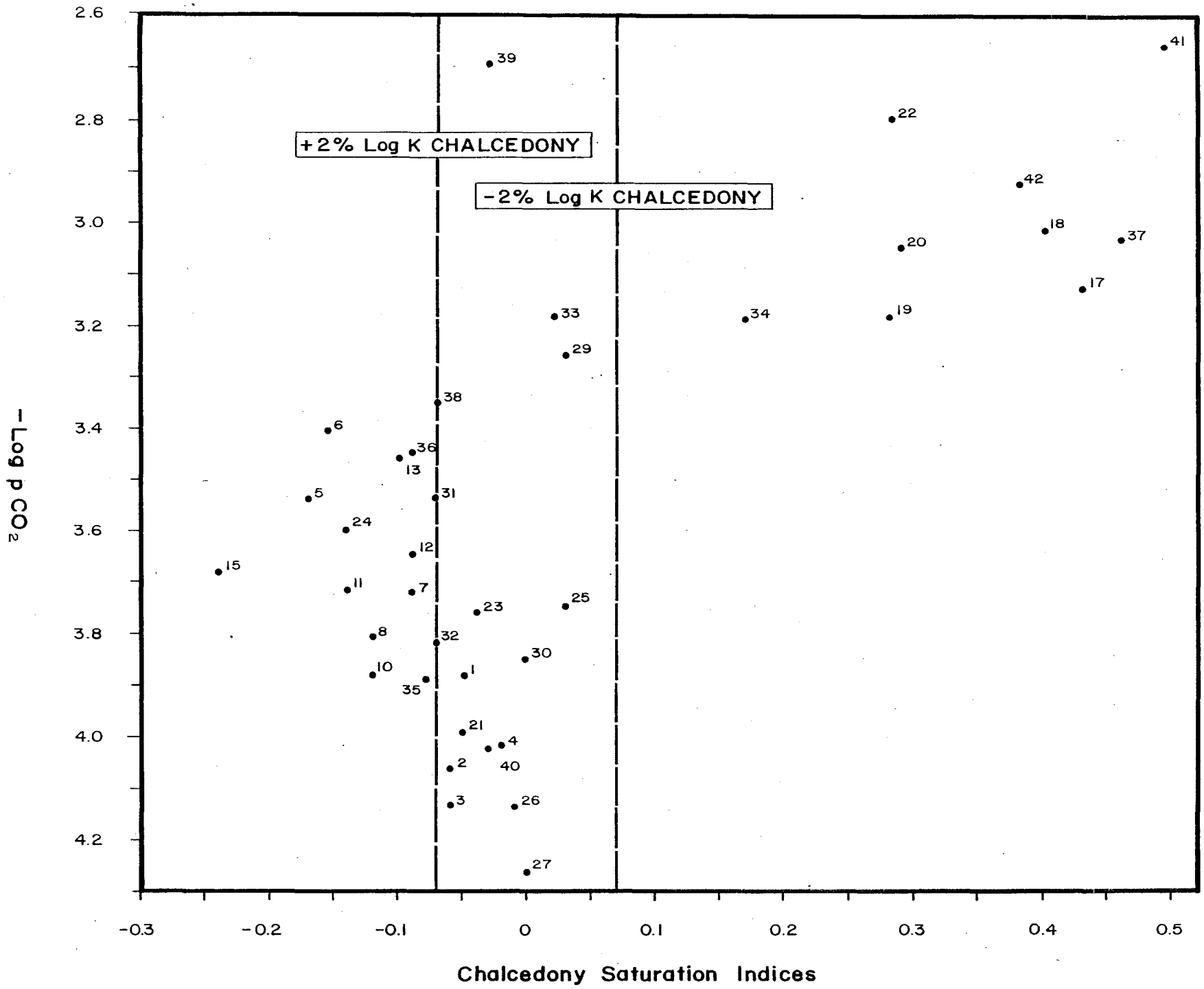

Figure 19 Chalcedony saturation indices versus $-\text{Log } pCO_2$ concentration

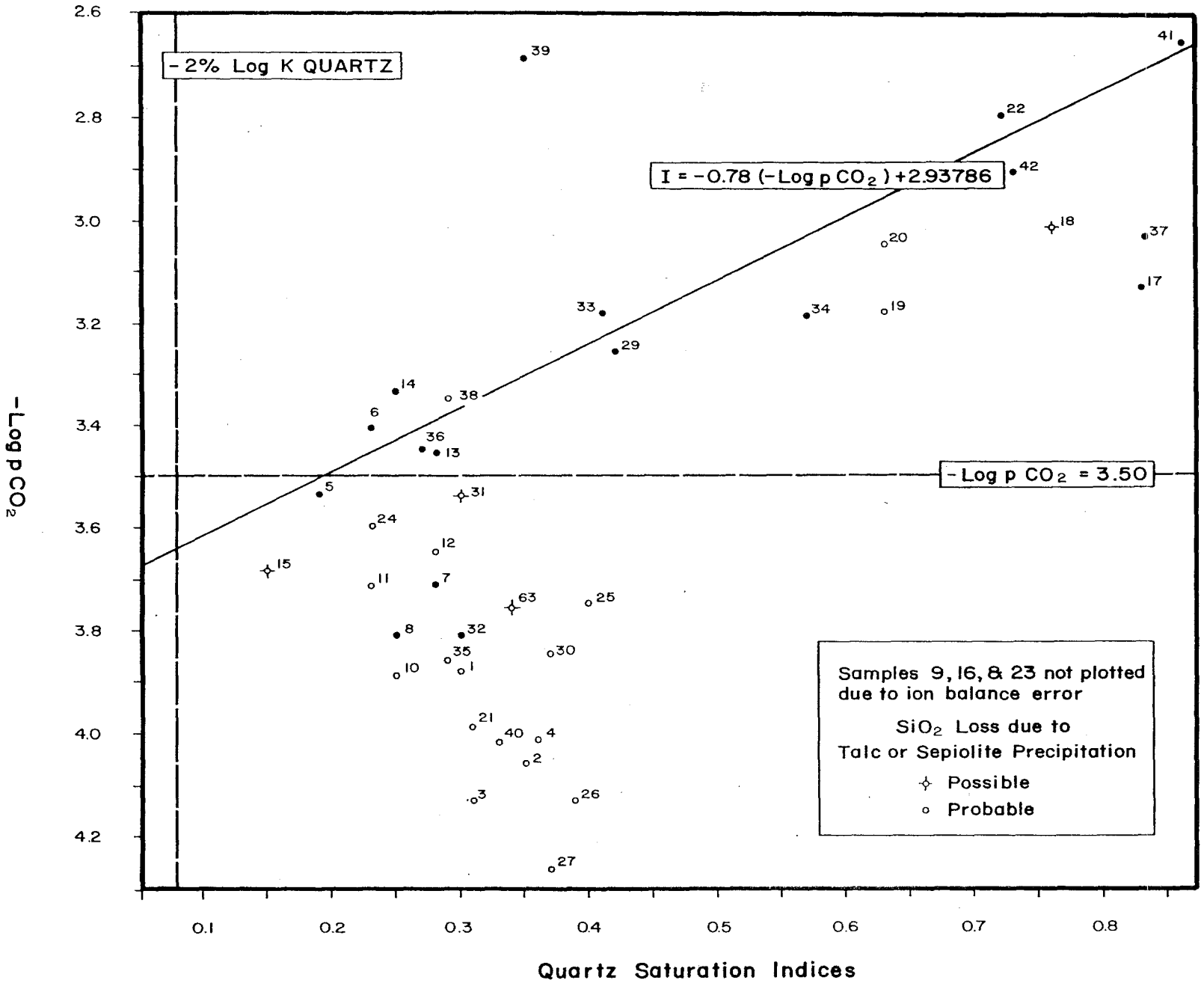

Figure 20 Quartz saturation indices versus -Log pCO_2 concentration

A CO2-CORRECTED QUARTZ GEOTHERMOMETER

Silica geothermometers are based upon experimental solubility of solid silica polymorphs at different temperatures. They were derived with plots of log silica concentration (log K) versus the inverse of absolute temperature (T). The equation is a variation of the familiar linear relationship describing a line:

Equation 42

$$1000/T = (m \log K) + b$$

where m and b are constants

We propose a correction to the silica geothermometer for ground water less than 100 C. This correction involves the use of a disequilibrium indices (I) that is determined from the relationship between quartz saturation indices and log pCO2 concentration. This factor I is subracted from log K in the pCO2 corrected geothermometer.

Equation 43

$$1000/T = (m \log K - I) + b$$

We use an upper limit of quartz saturation indices versus log pCO2 greater than -3.50 of samples from Cactus Flat to describe I (see Figure 20). Samples which are undersaturated with dolomite and saturated with talc (open symbols) are not used to describe this limit because they may have lost dissolved silica due to precipitation of magnesium silicate minerals. Also, samples 17, 37, and 39 are not used. Samples 17 and 34 are form Buena Vista. Sample 39 is unrepresentative of aquifer conditions (see section on interpretation of field studies). The equation describing this upper limit is:

Equation 44

APPLICATION OF THE NEW CO_2 CORRECTION TO THE QUARTZ GEOTHERMOMETERS AT CACTUS FLAT-ARTESIA AND BUENA VISTA

APPLICATION

A CO_2 correction to the quartz geothermometer was applied to waters having log pCO_2 greater than -3.50. This correction subtracts the non-silica polymorph dissolved fraction to allow realistic application of silica geothermometers to low temperature ground water. In other waters, with log pCO_2 less than -3.50, dissolved silica is in apparent equilibrium with chalcedony (Figure 19). Comparison of the CO_2 corrected geothermometer temperatures and the chalcedony temperatures with measured temperatures for the Cactus Flat-Artesia area shows that these geothermometers agree well with measured temperatures. This is expected because the Cactus Flat-Artesia samples are from confined aquifers.

We compared the results of a conventional resource assessment using Na-K-Ca and SiO_2 geothermometer temperatures calculated from published data with our CO_2-corrected silica geothermometer temperatures and chalcedony geothermometer temperatures calculated from water chemistry collected during this study. First, we reviewed the published water chemistry from Cactus-Artesia and Buena Vista and applied the conventional geothermometers to estimate reservoir temperatures (Table 4). Figures 21, 22, and 23 show that these geothermometers suggest a 80 to 100°C reservoir at Buena Vista and 80 to 90°C reservoir at Cactus Flat-Artesia. Second, we tabulated the silica geothermometer temperatures for water samples we collected (Table 5) and applied the CO_2 correction to those samples having log pCO_2 greater than -3.5. The correction was applicable to seven samples at Cactus Flat and five at Buena Vista.

These new values and the revised silica geothermometer maps (Figs. 24 and 25) suggest lower reservoir temperatures. A more realistic resource temperature at Buena Vista appears to be in the 50 to 70°C range, about 30 °C lower than predicted on the basis of an uncorrected silica geothermometer alone. A temperature-depth profile of a deep well 5km east of Buena Vista shows a temperature inversion at 500m (Reiter and Shearer,1979). This profile indicates the existance of a 65 to 70°C convective geothermal system in the Buena Vista area. The CO_2-corrected

TABLE 4 - Measured and Geothermometer Temperatures, Published Data, Cactus Flat-Artesia and Buena Vista

Location		Temp(°C)	TChal(°C)	TQtz(°C)	TNa-K-Ca(°C)
(D-8-25)	1ddd	36	31.4	63.4	81.0
	12aaa	39	26.5	58.7	94.3
	12aaa	39	45.0	76.6	75.7
	12aaa	39	31.4	63.4	95.6
(D-8-26)	6cbb	31	25.2	57.4	61.7 *
	7ab	45	31.4	63.4	83.6
	7ac	37	50.5	81.7	67.8
	7adc	32	20.5	53.0	85.5 *
	7ba	34.5	45.0	76.6	87.4
	7bb	33.5	45.6	78.0	68.0
	7bbb	34	27.3	59.5	93.3
	7da	41.5	45.0	76.6	86.7
	7dd	42	38.6	70.4	84.8
	7dda	39	28.3	60.5	87.5
	7dda	39	35.1	67.0	74.5
	7ddb	35	35.1	67.0	74.8
	7ddb	38	36.9	68.7	73.3
	8bdcc	39	18.3	50.8	92.2 *
	8ca	39.4	35.1	67.0	92.5
	9bc	29.4	48.1	79.4	51.9 *
	9bc	38.9	31.4	63.4	60.4 *
	19cdda	27	68.8	98.9	57.3
	19cddb	27	56.2	87.1	61.0
	19cddbc	29	53.5	84.6	66.9
	19dccb	27	71.9	101.8	52.6
	20cd	44	42.0	73.6	93.9
	20dbcc	45	28.1	60.3	105.2
	20dc	39.4	45.1	76.6	64.2
	32dcc	28	45.1	76.6	82.4
	33cccc	31	52.2	83.4	50.5
	33ccd	34	42.0	73.6	69.4
(D-9-26)	5ab	33	45.1	76.6	66.9
	5acb	33	46.6	78.0	64.3
(D-6-27)	35dddd	27	73.9	103.6	63.2 *
(D-7-27)	2aadc	36	45.1	76.6	66.2
	2aca	37.5	87.2	116.0	78.6 *
	2acb	38	82.1	111.3	67.9 *
	2adbb	40	43.5	75.1	29.2
	2add	41	85.5	114.5	73.3 *
	2addcb	39	83.9	113.0	127.6 *
	11bbb	43.5	87.2	116.0	75.8 *

* Mg correction applied

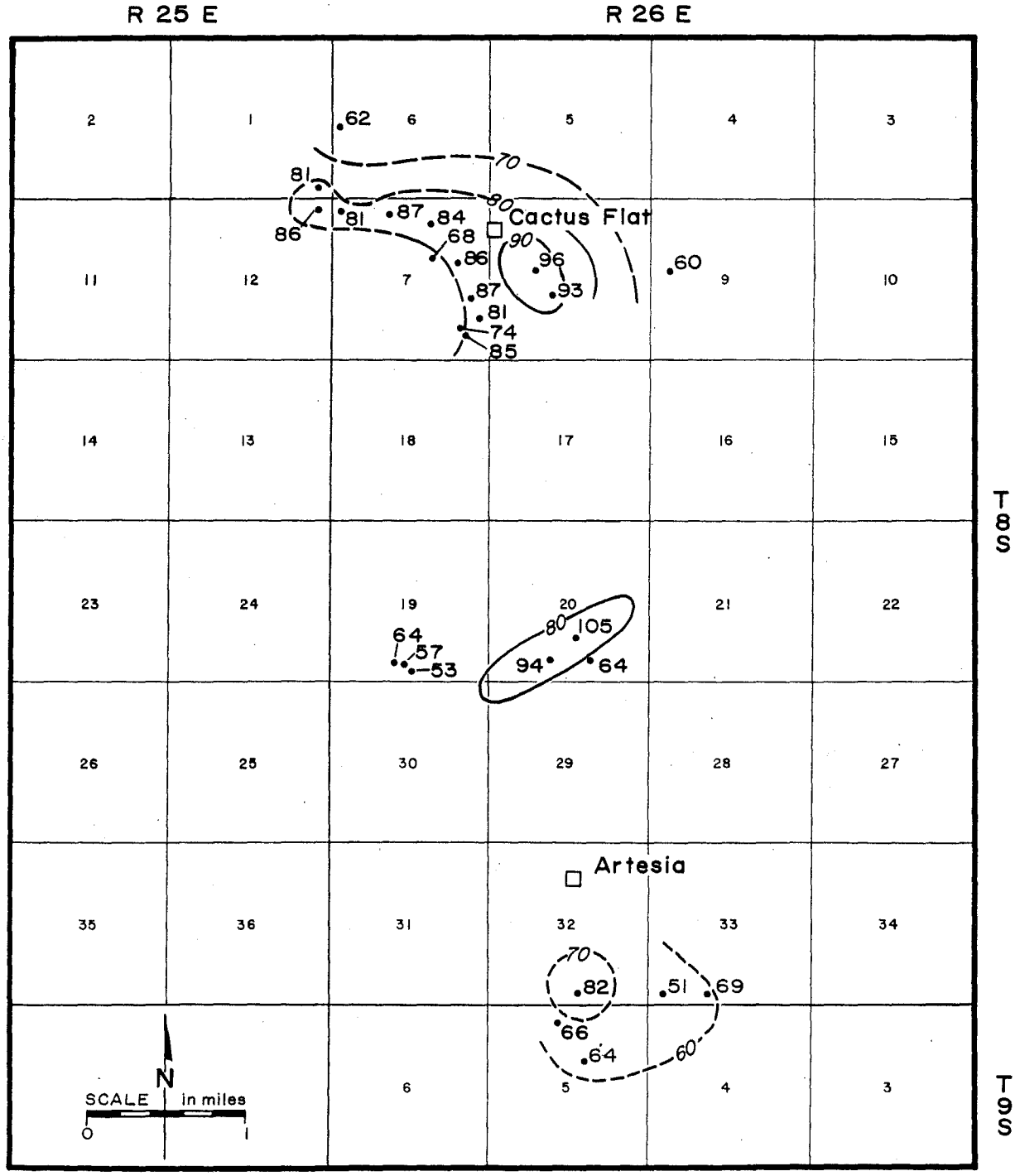

Figure 22 Map showing Na-K-Ca geothermometer temperatures calculated from published data at Cactus Flat-Artesia

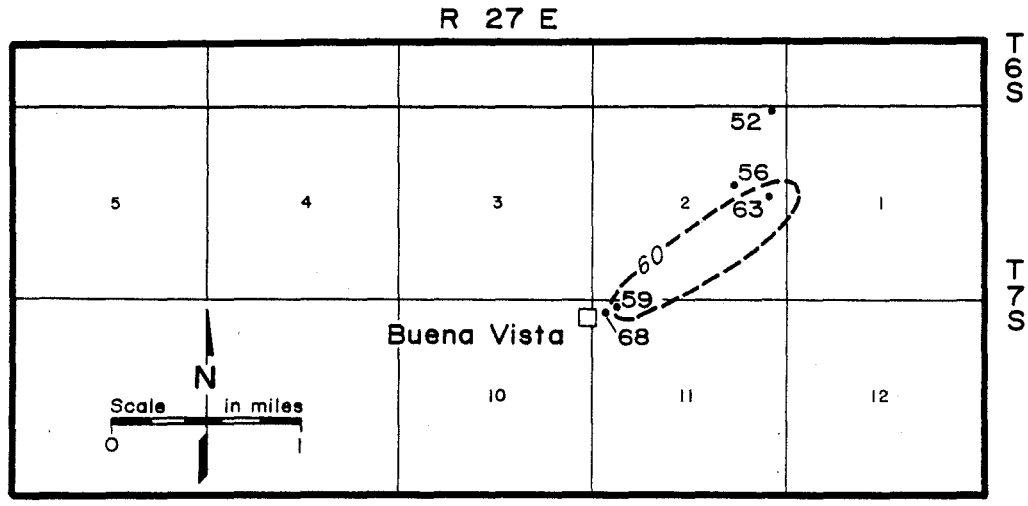

Figure 24 Map showing CO_2-corrected quartz geothermometer temperatures, this study, Buena Vists

TABLE 5 - Measured, SiO_2, and pCO_2-Corrected Geothermometer Temperatures, This Report, Cactus Flat-Artesia and Buena Vista

Location	Well No.	Temp(°C)	T_{Chal}(°C)	T_{Qtz}(°C)	T_{Qcorr}(°C)
(D-8-26) 7ddba	1W83	38.6	33.3	65.3	
7ddbc	2W83	34.6	33.3	65.3	
7bdab	3W33	34.3	33.3	65.3	
7bbcd	4W83	33.1	33.3	65.3	
7baac	5W83	41.4	25.2	57.4	
7adbc	6W83	29.2	15.4	48.0	30.8
7acad	7W83	35.3	29.4	61.5	
7acad	8W83	37.8	27.3	59.5	
7adcd	9W83	33.7	31.4	63.4	
7bbbc	10W83	33.8	22.9	55.3	
12aaaa	11W83	36.0	22.9	55.3	
12aaaa	12W83	38.5	29.4	61.5	
6ccba	13W83	30.4	22.9	55.3	40.5
7adcc	15W83	31.6	12.7	45.3	
(D-7-27) 2aaab	17W83	26.3	67.8	98.0	54.7
2acda	18W83	39.4	83.0	112.1	57.8
11bbbb	19W83	48.4	85.5	114.5	71.3
11bbbb	20W83	49.2	85.5	114.5	61.7
(D-8-26) 7bdbb	21W83	39.9	35.1	67.1	
(D-8-25) 27caaa	22W83	6.5	25.2	57.4	5.2
(D-8-26) 20dbbd	23W83	35.1	31.4	63.4	
20dbcb	24W83	38.7	27.3	59.5	
20dbca	25W83	36.5	38.7	70.4	
20acdb	26W83	33.7	35.1	67.1	
20acdb	27W83	38.0	42.0	73.6	
20adcc	29W83	26.5	27.3	59.5	31.9
18abdd	30W83	37.2	42.0	73.6	
18abdc	31W83	38.9	35.1	67.1	
17abbb	32W83	39.0	33.3	65.3	
8dcaa	33W83	26.6	27.3	59.5	27.2
8dcad	34W83	25.1	38.7	70.4	36.7
7dbda	35W83	41.3	35.1	67.1	
8bdcc	36W83	39.1	31.4	63.4	47.3
(D-7-27) 2addc	37W83	40.4	93.5	121.7	65.6
(D-8-26) 18addb	38W83	41.4	35.1	67.1	43.9
7bdbb	40W83	39.9	36.9	68.8	
(D-6-25) 23bbad	41W83	39.6	91.9	120.3	39.5
36cbbb	42W83	46.1	85.5	114.5	52.6

Bibliography - continued

Berner, R.A., 1980, Early Diagenesis, a Theoretical Approach: Princeton University Press, Princeton, N.Y., 241 p.

Berner, R.A., 1981. Kinetics of weathering and diagenesis: in Ribbe, P.H., ed., Kinetics of geochemical processes, Mineralogical Society of America, Reviews in Mineralogy, v. 8, p. 111-134.

Berner, R.A., and Holdren, G.R., Jr., 1977, Mechanism of feldspar weathering: some observational evidence: Geology, v. 5, p. 369-372.

Berner, P.A., and Holdren, G.R., 1979, Mechanism of feldspar weathering: II. observations of feldspars from soils: Geochimica et Cosmochimica Acta, v. 43, p. 1173-1186.

Bodvarsson, G., 1960, Exploration and exploitation of natural heat in Iceland: Bulletin Volcanologique, v. 23, p. 241-250.

Bricker, O.P., 1967, Cations and silica in natural waters: controls by silicate minerals: International Association Sci. Hydrology Publication 78, p. 110-119.

Bricker, O.P. and Garrels, R.M., 1967, Mineralogic factors in natural water equilibria in Faust, S.D., Hunter, J.U., eds., Principles and Applications of Water Chemistry: New York, Wiley, 643 p.

Bricker, O.P., Godfrey, A.E., and Cleaves, E.T., 1968, Mineral-water interactions during the chemical weathering of silicates: Trace Inorganics in Water. American Chemical Society Adv. Chemical Series 73, p. 128-142.

Brown, E., Skougstad, M.W., and Fishman, M.J., 1970, Methods for collection and analysis of water samples for dissolved minerals and gases: U. S. Geological Survey Techniques of Water Resources Investigation Book 5, Chapter A-1.

Busenberg, E., and Clemency, C.V., 1976, The dissolution kinetics of feldspars at 25°C and 1 atm CO_2 partial pressure: Geochimica at Cosmochimica Acta, v. 40, p. 41-49.

Butler, J.N., 1982, Carbon dioxide equilibria and their applications: Addison-Wesley Publishing Company, 259 p.

Crerar, D.A., and Anderson, G.M., 1971, Solubility and solvation reactions of quartz in dilute hydrothermal solutions: Chemical Geology, v. 8, p. 107-122.

Bibliography - continued

Dutt, G.R., and McCreary, J.W., 1970, The quality of Arizona's domestic, agricultural, and industrial waters: University of Arizona Agricultural Experiment Station Report 256, 83 p.

Ellis, A.J., and Mahon, W.A.J., 1977, Chemistry and Geothermal Systems: New York, Academic Press, 392 p.

Elston, W.E., 1958, Burro Uplift, northeastern limit of sedimentary basin of southwestern New Mexico and southeastern Arizona: American Association of Petroleum Geologists Bulletin, v. 42, p. 2513-2517.

E.P.A., 1976, Methods for chemical analysis of water and wastes: Environmental Protection Agency, Environmental Monitoring and Support Laboratory Cincinnati, Ohio.

Eyde, T.H., 1978, Bowie zeolite, an Arizona industrial mineral: Fieldnotes, Arizona Bureau of Geology and Mineral Technology, v. 8, No. 4, p. 1-5.

Feth, J.H., Roberson, C.E., and Polzer, W.L., 1964, Sources of mineral constituents in water from granitic rocks, Sierra Nevada, California and Nevada: U. S. Geological Survey Water-Supply Paper 1535-I, 70 p.

Fournier, R.O., 1973, Silica in thermal waters: laboratory and field investigations: Proceedings of International Symposium on Hydrogeochemistry and Biogeochemistry, Japan 1970, v. 1 Hydrogeochemistry: Washington, D.C., J.W. Clark, 122-139.

Fournier, R.O., 1977, Chemical geothermometers and mixing models for geothermal systems: Geothermics, v. 5, p. 41-40.

Fournier, R.O., 1979, Geochemical and hydrologic considerations and the use of enthalpy-chloride diagrams in the prediction of underground conditions in hot-spring systems: Journal of Volcanology and Geothermal Research, v. 5, p. 1-16.

Fournier, R.O., 1981, Application of water geochemistry to geothermal exploration and reservoir engineering: in Ryback, L. and Muffler, L.J.P., eds., Geothermal Systems: Principles and Case Histories, John Wiley and Sons LTD, New York, p. 109-143.

Fournier, R.O., 1983, A method of calculating quartz solubilities in aqueous sodium chloride solutions: Geochimica et Cosmochimica Acta, v. 47, p. 579-586.

Fournier, R.O. and Marshal, W.L., 1983, Calculation of amorphous silica solubilities at 25° to 300°C and apparent cation hydration numbers in aqueous salt solutions using the concept of effective density of water: Geochimica et Cosmochimica Acta, v. 47, p. 587-596.

Bibliography - continued

Garrels, R.M. and Howard, P., 1957, Reactions of feldspar and mica with water at low temperature and pressure: Clays & Clay Mineralogy, v. 2, p. 68-88.

Garrels, R.M. and Mackenzie, F.T., 1967, Origin of the chemical compositions of some springs and in lakes, in Equilibrium Concepts in Natural Water Chemistry: American Chemical Society Advances in Chemistry Series, v. 67, p. 222-242.

Garrels, R.M. and Thompson, G., 1962, A chemical model for seawater at 25°C and one atmosphere total pressure: American Journal of Science, v. 260, p. 57-66.

Goldich, S.S., 1938, A study in rock weathering: Journal of Geology, v. 46, p. 17-58.

Harbour, J., 1966, Stratigraphy and sedimentology of the upper Safford Basin sediments: unpub. PhD. thesis, University of Arizona, 242 p.

Heald, M.T., 1955, Stylolites in sandstones: Journal of Geology, v. 63, p. 101-114.

Helgeson, H.C., 1968, Evaluation of irreversible reactions in geochemical processes involving minerals and aqueous solutions: I thermodynamic relations: Geochimica et Cosmochimica Acta, v. 32, p. 853-877.

Helgeson, H.C., 1969, Thermodynamics of hydrothermal systems at elevated temperatures and pressures: American Journal Science, v. 267, p. 729-804.

Helgeson, H.C., 1970, Description and interpretation of phase relations in geochemical processes involving aqueous solutions: American Journal of Science, v. 268, p. 415-438.

Helgeson, H.C., 1971, Kinetics of mass transfer among silicates and aqueous solutions: Geochimica et Cosmochimica Acta, v. 35, p. 421-469.

Helgeson, H.C., 1972, Chemical interaction of feldspars and aqueous solutions, in Mackenzie, W.S., and Bussman, J., eds., The Feldspars (Proceedings, Nato Advanced Study Institute): Manchester, England, Manchester University Press, p. 184-217.

Helgeson, H.C., Brown, T.H. and Leeper, R.H., 1969, Handbook of Theoretical Activity Diagrams Depicting Chemical Equilibria in Geologic Systems Involving an Aqueous Phase at one atm. and 0° to 300°C: Freeman and Cooper, and Co., San Francisco, 253 p.

Helgeson, H.C., Brown, T.H., Nigrini, A. and Jones, T.A., 1970, Calcu-

Bibliography - continued

Kline, W.E., 1980, The catalyzed dissolution of silicate minerals by hydrofluoric acid: unpub. PhD. thesis, the University of Michigan, 237 p.

Knechtel, M.M., 1938, Geology and ground-water resources of the Valley of the Gila River and San Simon Creek, Graham County, Arizona: U. S. Geological Survey Water Supply Paper 796, p. 222.

Krauskopf, K.B., 1956, Dissolution and precipitation of silica at low temperatures: Geochimica et Cosmochimica Acta, v. 10, p. 1-26.

Krauskopf, K.B., 1959, The geochemistry of silica in sedimentary environments: in Silica in Sediments. Society of Economic Paleontologists and Mineralogists Special Publication No. 7, p. 4-19.

Land, L.S. and Milliken, K.L., 1981, Feldspar diagenesis in the Frio Formation, Brazona County, Texas Gulf Coast: Geology, v. 9, No. 7, p. 314-318.

Lasaga, A.C., 1981, Rate laws of chemical reactions, in Ribbe, P.H., ed., Kinetics of geochemical processes, Mineralogical Society of America, Reviews in Mineralogy, v. 8, p. 1-68.

Loughnan, F.C., 1969, Chemical weathering of the silicate minerals: American Elsevier Publishing Company, Inc., New York, 154 p.

Lloyd, R.M., 1968, Oxygen isotope behavior in the sulfate-water system: Journal of Geophysical Research, v. 73, p. 6099-6110.

Luce, R.W., Bartlett, R.W. and Parks, G.A., 1972, Dissolution kinetics of magnesium silicates: Geochimica et Cosmochimica Acta, v. 36, p. 35-50.

Mackenzie, F.T. and Gees, R., 1971, Quartz: synthesis at earth-surface conditions: Science, v. 173, p. 533-535.

Mahon, W.A.J., 1966, Silica in hot water discharged from drill holes at Wairakei, New Zealand: New Zealand Journal of Science, v. 9, p. 135-144.

Mahon, W.A.J., 1975, Review of hydrogeochemistry of geothermal systems - prospecting, development, and use: Proceedings 2nd United Nations Symposium on the Development and Use of Geothermal Resources, v. 1, p. 775-783.

Mazor, E., Levitte, D., Truesdell, A.H., Healy, J., and Nissenbaum, A., 1980, Mixing models and ionic geothermometers applied to warm (up to 60°C) springs: Jordan Rift Valley, Israel: Journal of Hydrology, v. 45, p. 1-19.

Bibliography - continued

Oppenheimer, J.M. and Sumner, J.S., 1981, Gravity modeling of the basins in the Basin and Range Province Arizona: in Stone, C. and Jenney, J.P., eds, Arizona Geological Society Digest, v. 13, p. 111-115.

Paces, T., 1972, Chemical characteristics and equilibrium in natural water -felsic rock-CO_2 system: Geochimica et Cosmochimica Acta, v. 36, p. 217-240.

Paces, T., 1973, Steady-state kinetics and equilibrium between ground water and granitic rock: Geochimica et Cosmochimica Acta, v. 37, p. 2641-2663.

Paces, T., 1975, A systematic deviation from Na-K-Ca geothermometer below 75° and above 10^{-4} atmo P_{CO_2}. Geochimica et Cosmochimica Acta, v. 39, p. 541-544.

Paces, T., 1976, Kinetics of natural water systems: Interpretation of Environmental Isotope and Hydrochemical Data in Groundwater Hydrology. International Atomic Energy Agency, Vienna, p. 85-108.

Paces, T., 1978, Reversible control of aqueous aluminum and silica during the irreversible evolution of natural waters: Geochimica et Cosmochimica Acta, v. 42, pp. 1487-1493.

Petrovic, R., Berner, R.A. and Goldhaber, M.B., 1976, Rate control in dissolution of alkali feldspars: I study of residual feldspar grains by X-ray photonelectron spectroscopy Geochimica et Cosmochimica Acta, v. 40, p. 537-548.

Pettijohn, F.J., Potter, P.E., Siever, R., 1973, Sand and Sandstones: Springer-Verlag, New York, 618 p.

Phoenix Geophysics Incorporated, 1979, Report on the reconnaissance resistivity and VLF-EM surveys of the Safford Valley area, Graham County, Arizona for State of Arizona Bureau of Geology and Mineral Technology: Arizona Bureau of Geology and Mineral Technology Open-File Report 81-23.

Plummer, L.N. and Back, W., 1980, The mass balance approach: application to interpreting the chemical evolution of hydrologic systems: American Journal of Science, v. 280, p. 130-142.

Plummer, L.N., Jones, B.F. and Truesdell, A.H., 1976, WATEQF - a FORTRAN IV version of WATEQ, a computer program for calculating chemical equilibrium in natural waters: U. S. Geological Survey Water Resources Investigations 76-13, 61 p.

Potter, R.W., Marshall, W.L., Fournier, R.O. and Martynoua, O.I., 1978, Bibliography of the available data on the solubility of silica in water substance: U. S. Geological Survey Open-File Report 78-731, 7 p.

Bibliography - continued

Siever, R., 1962, Silica solubility, 0-200°C, and the diagenesis of siliceous sediments: Journal of Geology, v. 70, p. 127-150.

Siffert, B., 1967, Some Reactions of Silica in Solution: Formation of clay: (translated from French by Israel Program for Scientific Translations and published for the U. S. Department of Agriculture and the National Science Foundation, Washington, D.C.) Universite De Strasbourg Memoires Du Service De La Carte Geologique D'alsace et De Lorraine No. 21, 100 p.

Silver, L.T., 1978, Precambrian formations and Precambrian history in Cochise County, southeastern Arizona: in Callender, J.F., Wilt, J.C. and Clemons, R.E., eds., Land of Cochise, New Mexico Geological Society Guidebook, 29th Field Conference, p. 231-241.

Smalley, R.C. and Long, A., 1983, An isotopic and geochemical investigation of the thermal waters in the Safford Basin, Arizona (abstract): Abstracts with Programs Rocky Mountain Section Annual Meeting of the Geological Society of America, p. 416.

Stumm, W. and Morgan, J.J., 1970, Aquatic Chemistry, An Introduction Emphasizing Chemical Equilibria in Natural Waters: New York, Wiley Interscience, 583 p.

Strangway, D.W., Simpson, J. and York, D., 1976, Paleomagnetic studies of volcanic rocks from the Mogollon Plateau area of Arizona and New Mexico: in Cenozoic Volcanism in Southwestern New Mexico: New Mexico Geological Society Special Publication 5, p. 119-124.

Struhsacker, E.M., Smith, C. and Capuano, R.M., 1983, An evaluation of exploration methods for low-temperature geothermal systems in the Artesia City area, Idaho: Geological Society of America Bulletin, v. 94, p. 58-79.

Swan, M.M., 1982, Influence of pre-Cretaceous structure upon Late Cretaceous-Tertiary magmatism in southern Arizona and New Mexico (abstract): Abstracts, 78th Annual Meeting, Cordilleran Section, The Geological Society of America, April 19-21, 1982, Anaheim, California, p. 238.

Swanberg, C.A., Morgan, P., Stoyer, C.H. and Witcher, J.C., 1977, An appraisal study of the geothermal resources of Arizona and adjacent areas in New Mexico and Utah and their value for desalination and other uses: New Mexico Energy Institute Report 6, New Mexico State University, 76 p.

Thomson, A., 1959, Pressure solution and porosity: in Ireland, H.A., ed., Society of Economic Paleontologists and Mineralogists Special Publication 7, p. 21-111.

Bibliography - continued

Weyl, P.K., 1959, Pressure solution and the force of crystallization - a phenomenological theory: Journal of Geophysical Research, v. 64, p. 2001-2025.

White, D.E., 1965, Saline waters of sedimentary rocks: American Association of Petroleum Geologists, Memior 4, p. 352-366.

White, N.D. and Smith, C.R., 1965, Basic hydrologic data for San Simon Basin, Cochise and Graham Counties, Arizona, and Hidalgo County, New Mexico: Arizona State Land Department Water Resources Report 21, 42 p.

Wigley, T.M.L., 1977, WATSPEC: A computer program for determining the equilibrium speciation of aqueous solutions: British Geomorphological Research Group. Technical Bulletin No. 20, Geo Abstracts LTD., University of East Anglia, Normich, England, 40 p. with computer listing.

Wildman, L.D., Jackson, M.L. and Whittig, L.D., 1968, Serpentine rock dissolution as a function of carbon dioxide pressure in aqueous solution: American Mineralogist, v. 53, p. 1250-1263.

Wirth, G.S., 1980, The heterogeneous kinetics of silica dissolution in aqueous media: unpub. PhD. thesis, University of California, San Diego, 182 p.

Witcher, J.C., 1979, A preliminary report on the geothermal energy potential of the Safford Basin southeastern Arizona: in Geothermal Site Evaluation in Arizona, Semi-annual Progress Report for Period July 1978 - January 1979, D.O.E. Contract EG-77-S-02-4362, p. 42-72.

Witcher, J.C., 1981, Geothermal resource potential of the Safford-San Simon Basin, Arizona: Arizona Bureau of Geology and Mineral Technology Open-File Report 81-26, 131 p.

Witcher, J.C., 1982, Exploration for geothermal energy in Arizona Basin and Range, a summary of results and interpretations of heat flow and geochemistry studies in Safford Basin, Arizona: Arizona Bureau of Geology and Mineral Technology Open File Report 82-5.

Wollast, R., 1967, Kinetics of the alteration of K-feldspar in buffered solutions at low temperature: Geochimica et Cosmochimica Acta, v. 31, p. 635-648.

Wollast, R., 1974, The silica problem, in Goldberg, E.D., ed., The Sea, v. 5, New York, Wiley-Interscience, p. 359-392.

Wynn, J.C., 1981, Complete Bouguer gravity anomaly map of the Silver City $1^{o}x2^{o}$ quadrangle, New Mexico - Arizona: Miscellaneous Investigations Series Map I-1310-A, 1:250,000 scale.